# LoI 00-002 and supplementary information

The improved text of the L0I 00-002.

The letter from B.Holstein.

The message from I.Khriplovich.

The Figure of Merit of proposed experiment.

The Expected time schedule of proposed experiment.

The Use of Rotating Target in proposed experiment.

Paper by E. Earle et al. about Chalk River experiment.

Paper by U. Meibner on theory review.

Review part of the LANL proposal by J.Bowman et al.

# Letter-of-Intent 00-002 for PAC 17

## Study of the Parity Non-Conserving Force between Nucleons through Deuteron Photodisintegration

Ch. Sinclair and B. Wojtsekhowski (co-spokesman), *JLab*
W.T.H. van Oers (co-spokesman) and R. J. Woo, *University of Manitoba*
W.M. Snow, *University of Indiana*
M.B. Leuschener, *University of New Hampshire*
J.D. Bowman, S.I. Penttila, and W.S. Wilburn, *Los Alamos National Laboratory*

## Introduction

The flavor conserving nonleptonic weak interaction, e.g., $np \rightarrow np$, is the last sector of the weak interaction where the main aspects of electroweak theory are not presently reproduced experimentally. The weak nucleon-nucleon interaction leads to a Parity Non-Conserving (PNC) force between nucleons. At low energy due to the heaviness of the W(Z) one can consider a pointlike weak interaction between quarks. Because of the strong repulsion between nucleons the probability of such an interaction is very low. A long range PNC nucleon-nucleon (NN) interaction arises from meson exchange with one of the quark-meson vertices containing a W(Z). The size of the PNC effect can be estimated as $G_F m_\pi^2 \sim 10^{-7}$. As the ordinary low energy NN interaction can be described by exchanges of mesons, the PNC interaction also can be presented as a sum of light meson exchanges. The form of the parity violating Hamiltonian is [1]:

$$
\begin{aligned}
H_{wk} &= \frac{f_\pi}{2}\overline{N}\,(\tau \times \pi)_3\, N \\
&+ \overline{N}\{h_\rho^0 \tau\cdot\rho^\mu + h_\rho^1\rho_3^\mu + \frac{h_\rho^2}{2\sqrt{6}}(3\tau_3\rho_3^\mu - \tau\cdot\rho^\mu)\}\gamma_\mu\gamma_5 N \\
&+ \overline{N}\{h_\omega^0\tau\cdot\omega^\mu + h_\omega^1\tau_3\omega_3^\mu\}\gamma_\mu\gamma_5 N - \overline{N}h_\omega^{\prime 1}(\tau\times\rho^\mu)_3\frac{\sigma_{\mu\nu}k^\nu}{2M}\gamma_5 N
\end{aligned}
\tag{1}
$$

There are seven weak coupling constants $f_\pi$, $h_\rho^0$, $h_\rho^1$, $h_\rho^2$, $h_\omega^0$, $h_\omega^1$, and $h_\omega^{\prime 1}$. A comprehensive calculation of these parameters was performed by Desplanques, Donoghue, and Holstein (DDH) in 1980 [2]. In their calculation DDH suggested "best" values and set the ranges of reasonable values for each of the weak meson-nucleon coupling constants. Later works [3] reevaluated the calculation of $f_\pi$, the longest range component of the weak NN interaction, and came to very different results.

The structure of the Hamiltonian, which is based on electroweak theory, leads to links between PNC observables in different reactions such as neutron capture by the proton, polarized-proton scattering from protons and very-light nuclei, gamma transitions in nuclei,

and so on. Tests of these links are in turn the tests of electroweak theory predictions, see also ref. [4].

The two parameters, $f_\pi$ and $h_\rho^0$, are the most important ones in many observables. Experimental information on $f_\pi$ comes mainly from measurements performed on nuclei whose interpretation is controversial. The value of $f_\pi$ extracted in ref. [5] from the experimental value of the anapole moment of $^{133}Cs$ [6] is twice as large as the "best guess" given by DDH. At the same time, the measurement of the circular polarization of the 1081 keV transition in $^{18}F$ [7], where the factors of the matrix elements (needed to extract $f_\pi$) were measured experimentally, led to an upper limit on $f_\pi$ three to four times less than the value predicted by DDH, see ref. [8]. A recent analysis [9] pointed out that uncertainties in the experimental value of $h_\rho^0$ makes the extraction of $f_\pi$ from the anapole moment of $^{133}Cs$ problematic. Measurements in the np system [10, 11, 12] were statistically limited. They yielded null results with error bars much larger than the theoretical uncertainties in the $f_\pi$ and $h_\rho$ couplings.

The approved LANSCE experiment $\vec{n}p \to d\gamma$ will measure $f_\pi$ through the correlation $A_\gamma$ of the photon emission and neutron spin directions. The expected asymmetry $A_\gamma$ is $\sim 5 \cdot 10^{-8}$ for the suggested DDH value for $f_\pi$. Experiments on $\vec{p}p$ scattering [13] under way at a proton energy of 221 MeV will be able to measure a combination $h_\rho^{pp} = h_\rho^0 + h_\rho^1 + h_\rho^2/\sqrt{6}$ .

The goal of the proposed experiment is also a determination of the pion-nucleon PNC coupling constant $f_\pi$ . We suggest using the PNC effect in the total cross section of deuteron photodisintegration which can be observed with circularly polarized photons. At threshold, the helicity correlated asymmetry is mostly sensitive to $h_\rho$, but for a photon energy $\sim 10$ MeV the contribution from $f_\pi$ dominates [14].

The deuteron has played an important role in the study of the nucleon-nucleon interaction for many years. One example is the T20 saga which lasted for twenty years from the first pion scattering experiment until the JLab measurement in 1997. The deuteron is also very useful for studying the weak nucleon-nucleon interaction because of its simple and well understood structure. The calculations [15] of the PNC asymmetry in the total cross section of the $d(\vec{\gamma}, n)p$ reaction with the DDH "best guess" coupling constants predict $A_z \sim 2.5 \cdot 10^{-8}$ at $E_\gamma \sim 10\ MeV$.

Our plan is to use a bremsstrahlung beam with an intensity of $\sim 10^{15}$ photons per second with energies above the deuteron breakup threshold, which leads to a statistical accuracy on the level of $1 \cdot 10^{-9}$ after one month of data taking.

The purpose of this Letter-of-Intent is to solicit the evaluation of a new line of research before investing the large effort required in developing a full proposal. The development of a full proposal will include detailed feasibility tests, which take little beam time but considerable preparation time. Also, execution of the experiment involves the addition of major new experimental apparatus. At this early stage, we are seeking feedback on the scientific merits and technical feasibility of the proposed research. The high photon flux available at JLab suggests the possibility of using the deuteron as a laboratory for studying the np weak interaction far above threshold region.

## The previous experiment on deuteron photodisintegration

The Chalk River experiment [12] was the only study of parity violating effects in the total cross-section of deuteron photodisintegration near threshold. The experimental uncertainty in this experiment was on the order of $10^{-6}$, which is too big to observe the PNC effect. However, the experiment did solve the discrepancy problem between the theoretical expectation and the first result from the inverse reaction [16]. The major contributors to the error budget were the fluctuations in beam energy and position.

## Experimental considerations

A uniquely stable highly polarized electron beam has been developed at JLab. The systematics in a recent PNC measurement was about $10^{-8}$ for $P_e \sim 40\%$ [17]. In the past year a great deal has been learned about running with strained GaAs. Techniques have been developed to reduce helicity correlated beam parameters while running with high polarization. During the 1999 HAPPEX run the corrections due to beam parameters were in the worst case $\sim 5 \cdot 10^{-8}$ and $P_e \sim 70\%$. These developments are being continued by the polarized injector group in collaboration with the G0 and HAPPEX II experimenters. Stability of the beam energy on the level of a few times $10^{-6}$ has become routine and ways for further improvement are under study. The beam polarization is now typically twice as high as in earlier days. Beam position jitter is on the order of 100 nm. So, we have a much improved situation for a second measurement of the PNC effect in the $d(\vec{\gamma}, n)p$ process. In Fig. 1 we present a schematic view of the setup. Below we outline the major parameters of the proposed apparatus:

- the beam polarization $P_e$ is $\sim$ 80%.
- the beam current is $\sim 1\, mA$.
- the beam energy is $3 \div 8$ MeV.
- the beam energy is analyzed in a magnet with 50 cm radius.
- the beam position and direction are measured by cavity based BPMs.
- the beam spot size is 2 mm, achieved by use of the rastering scheme.
- the photon production target is made of 0.75 mm gold plate.
- the 25-cm long liquid deuterium target ($LD_2$) takes about 50 W.
- lead shielding will reduce the intensity of the scattered photons on the neutron detectors.
- a heavy water moderator will be used to slowdown the neutrons.
- the main detector is located at a distance of 1 meter from the $LD_2$ target.
- the main detector has two components, a first, which is sensitive to slow neutrons, and a second, which is sensitive only to photons.
- the photon detectors located in the forward direction will be used to measure the intensity and angular distribution of the photon beam.
- additional ( Compton ) detectors will be installed between the $LD_2$ target and the lead shield. They will be used to measure the PNC effect in Compton scattering from atomic electrons which is very small and can be calculated exactly. Use of the aerogel radiator with

refraction index n, for example 1.01, allows discrimination of the contribution of the photons with energy below 3.5 MeV.

• the main detector has segmentation in the forward and the backward parts in order to give sensitivity to the directional asymmetry in addition to the PNC asymmetry in the total cross section.

The expected high counting rate of the neutron detectors ( $\sim 10^{12}$ Hz ) will aid in the study of tiny systematics effects. The statistical accuracy will be $\sim 6$ *ppm* in a 30 ms period. However, the choice of spin flip frequency needs to be optimized to minimize fluctuations of the beam energy and position. Modulation techniques, developed in [18], will be used for the measurement of the rate variations with beam energy and position. The accuracy of these corrections are expected to be a dominant part of the error budget.

We performed a MC simulation of the experiment using GEANT, which took into account production of the photons in the radiator, polarization transfer from the electron to the photon, the deuteron photodisintegration cross section, and the energy dependence of the PNC asymmetry. The simulation supports the expectation that at higher beam energies photon production becomes much more efficient. However, the average polarization of the photon becomes smaller. A Figure-of-Merit (FOM1) was defined as the number of photons above the deuteron breakup threshold ($N_\gamma$) multiplied by the product of the disintegration cross section, the square of the photon polarization transfer coefficient, and the square of the PNC asymmetry, averaged over the photon spectrum ($\overline{\sigma_{\gamma,n} \cdot (P_\gamma/P_e)^2 \cdot A_z^2}$) The material of the radiator was chosen for maximum FOM1, which leads to larger Z and higher photo neutron threshold ($E_{th}$). The maximum beam energy was chosen right below $E_{th}$. We found that a gold radiator is the best choice.

The Figure-of-Merit of the experiment, which is the product of the FOM1 defined above and the square of $P_e$, is expected to be a factor of 50 higher than in the previous experiment [12]. The best estimate for the amount of beam time required for the production run is approximately two weeks. Only a few days of data taking be required by neutron statistics. However, measurements necessary to have systematics under control will take much longer.

## Conclusion

The PNC experiments at low energy have received much attention in recent years [19]. The determination of the coupling constants of the weak nucleon-nucleon interaction will establish a link between atomic, nuclear, and nucleon-nucleon parity violation experiments. Improvements in the beam polarization and the experimental arrangement provide a gain in the Figure-of-Merit by a factor of 50 compared to the previous deuteron photodisintegration experiment. Monitoring of the helicity asymmetry of the Compton scattered photons will be used as a null effect for control of the experimental systematics. It is expected that measurements of $f_\pi$ on the level of accuracy of 30% of the "best" DDH value can be made using only moderate beam time.

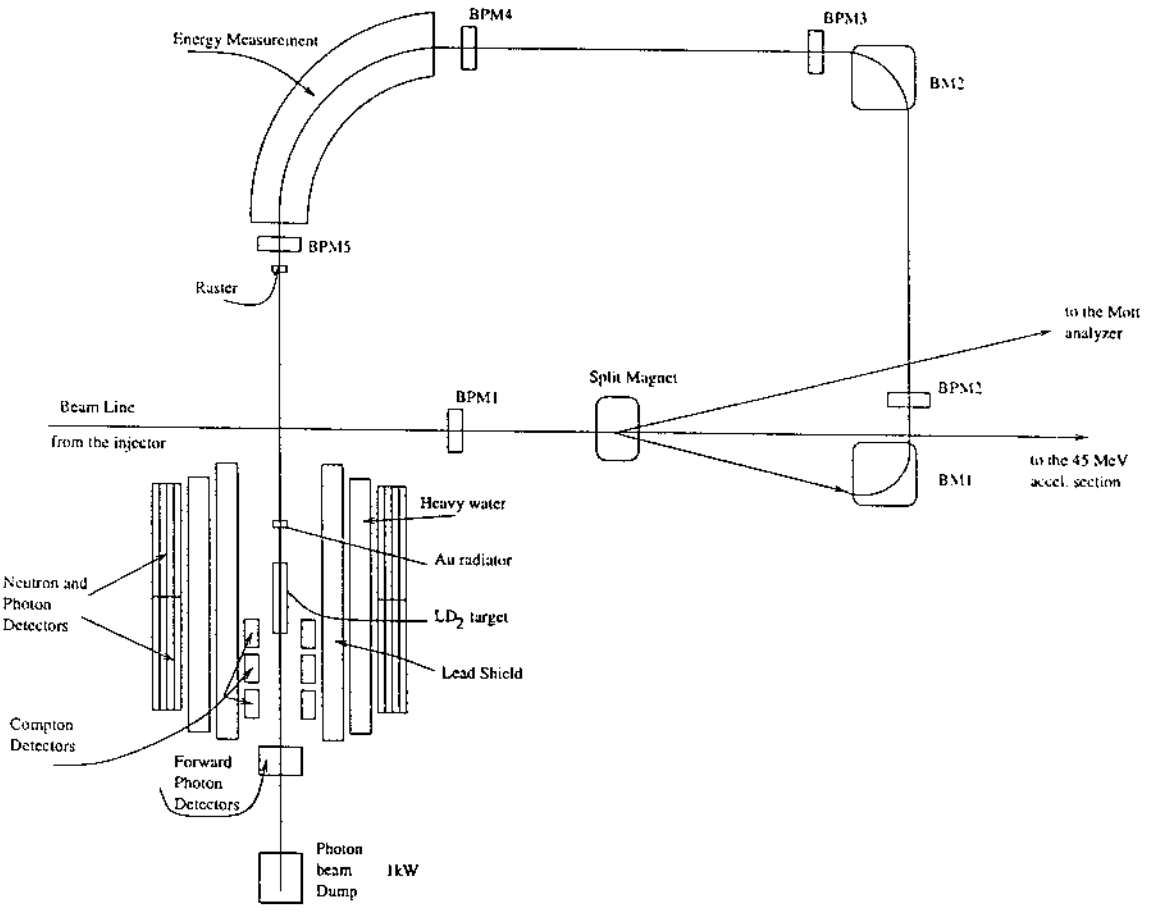


Figure 1: Proposed experimental setup for study $d(\vec{\gamma}, n)p$. BM1-BPM5 are cavity based beam position monitors; BM1, BM2 are the bending magnets. Compton Detectors are used for monitoring of the helicity asymmetry in scattering of the photons from the atomic electrons.

# References


[1] W. Haeberli and B. Holstein, in *Symmetries and Fundamental Interactions in Nuclei*, edited by W.Haxton and E.Henley ( World Scientific, Singapure, 1995), p.17.

[2] B. Desplanques, J. Donoghue, and B. Holstein, Ann. Phys. **124**, 449 (1980).

[3] E.M.Henley, W-Y.P.Hwang, and L.S. Kisslinger, Phys.Lett. B **367**, 21 (1996); D.B. Kaplan and M.J. Savage, Nucl. Phys. **A556**, 653 (1993).

[4] J.D. Bowman (Spokesman) et al., Measurement of the Parity-Violating Gamma Asymmetry $A_\gamma$ in the Capture of Polarized Cold Neutrons by Para-Hydrogen, $\vec{n} + p \rightarrow d + \gamma$, proposal to DOE, 17 April 1998.

[5] V.V. Flambaum and D.W. Murray, Phys.Rev. C **56**, 1641 (1997).

[6] C.S. Wood et al., Science **275**, 1759 (1997).

[7] S.A. Page et al., Phys.Rev. C **35**, 1119 (1987); M.Bini et al., Phys.Rev. C **38**, 1195 (1988).

[8] E.G. Adelberger and W.C. Haxton, Ann.Rev.Nucl.Part.Sci. **35**, 501 (1985).

[9] W.S. Wilburn and J.D. Bowman, Phys.Rev. C **57** 3425 (1998).

[10] J.F. Caviagnac, B.Vignon, and R.Wilson, Phys.Lett. B **67**, 148 (1977).

[11] V.A. Knyaz'kov et al., Nucl. Phys. **A417**, 209 (1984).

[12] E.D. Earle et al., Can. J. Phys., **66**, 534 (1988).

[13] S.A. Page, in *"7th Intl. Conf. on Polarization Phenomena in Nuclear Physics"* , eds. A. Bourdard and Y. Terrien (Colloque de Physique 51, 1990) C6-253; W.T.H van Oers, in *"Future Directions in Particle and Nuclear Physics at Multi-GeV Hadron Beam Facilities"*, ed. D.F.Geesaman (BNL Report BNL-52389, 1993) p.161.

[14] Ulf-G. Meibner, Modern Physics Letters A **5**, 1703 (1990).

[15] Takamitsu Oka, Phys. Rev. D **27**, 523 (1983).

[16] V.M. Lobashov et al., Nucl. Phys. **A197**, 241 (1972).

[17] K.A. Aniol et al., Phys.Rev.Lett. **82**, 1096 (1999).

[18] P.A. Souder et al., Phys. Rev. Lett. **65**, 694 (1990).

[19] *NSAC long range plan (1999), The Weak Interaction within the Nuclear Environment*, pages 146-147.

**Support for JLab LOI 00-002**

Barry R. Holstein
University of Massachusetts

I basically agree with the introductory sentence of this LOI—"The flavor conserving nonleptonic weak interaction...is the last sector of the weak interaction where the main aspects of electroweak theory are not presently reproduced experimentally." This is certainly not for lack of trying. Indeed numerous experiments have attempted to probe this sector for nearly four decades and there have been corresponding theoretical efforts. including our own—Desplanques, Donoghue, and Holstein, Ann. Phys. (NY) **124**, 449 (1980). Reviews of the basic state of the field have been given by Adelberger and Haxton in Ann. Rev. Nuc. Part. Sci. **35**, 501 (1985) and by Haeberli and myself in the volume **Symmetries and Fundamental Interactions in Nuclei**, ed. W. Haxton and E. Henley, World Scientific, Singapore (1995).

It is generally agreed that one should be able to represent the low energy parity-violating NN interaction in terms of a meson-exchange approach in parallel with that used to describe its parity-conserving counterpart. Once this is accepted, the effective PV interaction must be describable in terms of just seven weak couplings, as given in Eq. 1 of the LOI, and of these $h_\rho^0$ and $f_\pi$ are dominant. Many of the previous experiments in this realm have used nuclei in order to amplify the parity violating signal. This amplification is possible due to the mixing which occurs when one has nearly degenerate same spin but opposite parity states. Unfortunately this increase in signal brings along with it a corresponding increase in "noise," in the form of nuclear physics complications, and we now have the situation that there exist a number of determinations of these weak coupling which are in serious disagreement with one another. Actually, things are not quite so bleak. Indeed in the case of $h_\rho^0$ low energy experiments in the $\vec{p}p$ sector (including the soon to be completed TRIUMF 221 MeV measurement) have converged on a value only slightly smaller than and of the same sign as the DDH best value, so this at least seems secure. Where the problems have arisen in for the $\Delta I = 1$ coupling $f_\pi$. In this case the beautiful anapole moment measurement by the Weiman group in Colorado suggests a "large" value consistent with the DDH best value prediction, while measurements of the circular polarization in the decay of the 1.081 MeV excited state of $^{18}F$ suggest a much smaller number. (Earlier measurements involving $^{21}Ne$ are consistent with the DDH value,

but these are clouded by nuclear physics uncertainties.) The only way out of this quagmire seems to be a measurement in a fundamental system such as $np$—*i.e.* the deuteron photodisintegration experiment proposed in this LOI or its time reversed analog, the $\vec{n}p \to d\gamma$ radiative capture experiment to be done at LANL. It has long been known that such measurements are primarily sensitive to $f_\pi$ and indeed a previous attempt to extract $f_\pi$ via deuteron photodisintegration was made at Chalk River. Unfortunately, the predicted size of the effect ($\sim 5 \times 10^{-8}$) requires heroic measures that until recently were not possible. Fortunately things have changed and the confluence of measurments at LANL via radiative capture and at JLab via photodisintegration should (let's hope they agree!) finally be able to put this problem to rest. Both efforts have my enthusiastic and unqualified support.

Amherst, MA
January 13, 2000

From I.B.Khriplovich@inp.nsk.su Wed Dec 29 09:54:34 1999
Date: Mon, 27 Dec 1999 10:19:50 +0600
From: Iosif B. Khriplovich <I.B.Khriplovich@inp.nsk.su>
To: Bogdan Wojtsekhowski <bogdanw@jlab.org>
S ect: Re: D(g,n)p

Dear Bogdan,

It is certainly extremely important to measure the weak pion-nucleon coupling constant, even with an accuracy of 20-30%. The point is that direct nuclear measurements (with fluorine) give an upper limit on it on the level of about 0.3 of the so-called "best value" while the atomic result for the ^{133}Cs anapole moment strongly support the "best value".

Yulik

# Figure of Merit for Study of the Parity Non-Conserving Force

Ch. Sinclair, B. Wojtsekhowski, *JLab*, W.T.H. van Oers, R. J. Woo, *University of Manitoba*, W.M. Snow, *University of Indiana*, M.B. Leuschener, *University of New Hampshire*, J.D. Bowman, S.I. Penttila, and W.S. Wilburn, *Los Alamos National Laboratory*

We present a comparison of the Figure of Merits for the proposed study of $f_\pi$ by using the $d(\vec{\gamma}, n)p$ reaction [1] and for the experiment under way at LANSCE using the reaction $\vec{n}p \to d\gamma$ [2].

| | | |
|---|---|---|
| type of an initial beam..... | electrons (CEBAF injector)..... | protons (LANSCE ring) |
| beam energy, MeV | 8 | 800 |
| beam polarization | 80% | - |
| average beam current | 1 mA | 200 $\mu$A |
| product | photons | neutrons |
| flux, per second | $1.4 \cdot 10^{15}$ | $3.8 \cdot 10^{10}$ |
| aver. polarization | 48% | 65% |
| flux on the target | $8.9 \cdot 10^{14}$ | $1.5 \cdot 10^{10}$ |
| reaction | $d(\vec{\gamma}, n)p$ | $\vec{n}p \to d\gamma$ |
| reaction absorb. length, cm | $1.4 \cdot 10^4$ | 14 |
| target | $LD_2$, 30 cm | $LH_2$, 30 cm |
| reaction yield, Hz | $1.9 \cdot 10^{12}$ | $1.5 \cdot 10^{10}$ |
| detector type | $^{10}B$ | CsI |
| detector efficiency | 50% | 100% |
| detector rate, Hz | $1.0 \cdot 10^{12}$ | $0.5 \cdot 10^{10}$ |
| aver. physics asymmetry | $1.3 \cdot 10^{-8}$ | $5 \cdot 10^{-8}$ |
| aver. experimental asym. | $6.2 \cdot 10^{-9}$ | $3.3 \cdot 10^{-8}$ |
| statistics needed for 100% accuracy result | $2.6 \cdot 10^{16}$ | $1 \cdot 10^{15}$ |
| time DAQ for result with 100% accuracy, seconds | $2.6 \cdot 10^4$ | $2 \cdot 10^5$ |

The comparison shows that the Figure of Merit for the JLab's proposal is $\sim 7$ times higher than the one for the LANSCE measurement.. The LANSCE experiment has the important advantage of higher experimental asymmetry. At the same time the pulsed regime of the neutron source has a potential disadvantage. We find both approaches are comparable and because the techniques are very different the measurements will be complementary.

[1] JLab LoI 002-00, B. Wojtsekhowski and W.T.H. van Oers (spokepersons) et al..

[2] J.D. Bowman (Spokesman) et al., Measurement of the Parity-Violating Gamma Asymmetry $A_\gamma$ in the Capture of Polarized Cold Neutrons by Para-Hydrogen, $\vec{n} + p \to d + \gamma$, proposal to DOE, 17 April 1998.

# Expected time schedule in development of the low energy parity experiment (LoI 002 00 )

Ch. Sinclair, B. Wojtsekhowski, *JLab*, W.T.H. van Oers, R. J. Woo, *University of Manitoba*, W.M. Snow, *University of Indiana*, M.B. Leuschener, *University of New Hampshire*, J.D. Bowman, S.I. Penttila, and W.S. Wilburn, *Los Alamos National Laboratory*

We like to present here our expectation of the time line for the measurement of the weak coupling constant $f_\pi$ at JLab.

We hope to get support of PAC 17 on the proposed direction of research and begin development in year 2000. During this year we like to study the spectrum of signal variations in a CEBAF injector tunnel. The helicity correlated and uncorrelated fluctuations are presently the main concern.

We plan to use current-to-frequency conversion on the PMT base and optical transmission to the DAQ system. These tests don't need any dedicated beam time.

The same year we like to make an experimental study of the stability of the beam energy and position following the 5 MeV accelerator section.

By the fall of 2000 we like to prepare a proposal for an engineering experiment. In that experiment we will use a 20-50 $\mu A$ electron beam, produce photons, and register Compton scattering from atomic electrons at large angles. In many aspects such a study will be similar to the final setup but doesn't require the large beam current, the cryogenic target, and the neutron detectors. So, we hope to submit such proposal in about one year time.

Depending on the progress in realization of the first experiment the proposal for the actual measurement could be submitted in 2003 - 2004.

# Use of Rotating Target Cooled by Thermal Radiation Heat Exchange In the GDNP Experiment

P. Degtiarenko, Rad. Con. Group
Jefferson Lab

## Gold target for the GDNP proposal

The proposed model of the photon production target is made of 0.75-mm Au plate mounted on 1-cm Al plate. 1 mA, 8-MeV electron beam is directed onto the gold plate to generate energetic photons; the aluminum support serves as stopper for low energy residual electrons, and also as heat absorber and conductor. This note discusses qualitatively, and gives some estimates of thermal characteristics of the target assembly in the conditions of high beam current concentrated in a small ($1\times1$ mm$^2$) area without rastering.

### Qualitative considerations

Thermoconductivity of gold = 3.18 [W*cm/cm$^2$/K] which means that difference of temperatures 1 K between two parallel 1 cm$^2$ surfaces 1 cm apart will produce power transfer 3.18 W. Of 8 kW in the beam approx. 5 kW are deposited in the gold plate. If we assume the heated volume as 1 mm$^3$, and take the distance to the cold layer as 1 mm, then power transfer is approximately $P = 1.5*(T_{hot}-T_{cold})$. To dissipate 5000 Watt we would need more than 3000 K temperature difference.

### GEANT model

Fig. 1 shows a simple target model made using GEANT simulation package. Sample interactions of 8 MeV electron beam with Gaussian (0.5 mm $\sigma$'s) transverse distribution are also shown. It can be seen from the figure that beam electrons are completely stopped in the target, and that the heat deposition by the beam is quite localized.

Fig. 2 shows calculated power distribution in the target for 1 mA beam current. Out of 8 kW delivered by the beam, 5.7 kW is deposited in the target locally, of which almost 5 kW are deposited in the gold plate in a volume less than 1 mm$^3$.

Realistic calculation for the Au on Al setup gives temperature rise to ~2500 K in 0.1 sec, and saturates at ~3500K. If one forces temperature of the back surface of the gold plate to be 300 K (see Fig. 3 for illustration to the temperature distribution in this case), then the equilibrium temperature at the front surface reaches 1270K, still very close to the melting point of gold (1337 K). Aluminum melts at 933 K which makes the case even more difficult.

Thus, it seems it is impossible to design Au/Al target capable to withstand the heat loads caused by such beam, without either rastering the beam, or moving the target.

## The method of rotating target

Beam rastering is the common practice solution dealing with high local power deposition in the accelerator beam interaction with targets. However, the rastering technique is limited because it is not always possible to increase the area covered by rastered beam at the target face enough to be able to dissipate all the heat. Also, large beam rastering could be source of systematic errors in many experiments and cause elevated experimental and environmental radiation backgrounds.

The **Rotating Target** device is proposed for use in the accelerator applications where large local power deposition in the target is expected and where beam rastering is either undesirable or impossible, or does not solve the problem. The scheme of the device is utilizing the method of **Moving Target** and the method of **Radiation Heat Exchange**, which are presented in the Jefferson Lab Invention Disclosure statements submitted for U.S. patents in parallel with the **Rotating Target** device in October 1999. Schematic drawing is shown in Figure 4.

The target takes shape of a flat ring with a constant thickness installed around the outer diameter of a thick metal cylinder playing the role of a 'heat sink'. The cylinder is mounted on two bearings and can be rotated by the induction coils around the cylindrical pipe. The flow of water coolant keeps the pipe cold. The bearings and the induction coils should be separated from the hot parts by the isolating inserts (made of ceramics or other heat-resistant material). The two **Sets of Parallel Plate Fins** are attached to the inner diameter of the cylinder and to the outer diameter of the pipe and inserted between each other as shown. All materials participating in the heat exchange assume good thermal conductivity. When accelerator beam hits rotating target, the heat is evenly distributed around the whole target ring and transferred to the heat sink.

The **Hot Parallel Plate Fins** positioned between the **Cold Parallel Plate Fins** radiate the heat flux $H = F_{rad}\, S\, \sigma\, (T^4_{hot} - T^4_{cold})$, where $F_{rad}$ is a coefficient dependent on the plate surface properties; S is radiating area; $\sigma$=5.7 $10^{-12}$ W $cm^{-2}$ $K^{-4}$ is the Stefan-Boltzmann constant; T is temperature in °K.

If we neglect $T_{cold}$, and assume for a simple exercise the equilibrium temperature of the heat sink to be 1000 °K, outer radius of the coolant pipe 2 cm, inner radius of the heat sink 10 cm, $F_{rad}$ conservatively as 0.3, then the heat flux exiting one hot fin equals approximately $0.3 \times 600 cm^2 \times 5.7\ 10^{-12} \times 1000^4$ which is about 1 kW, if one assumes that the heat flux at this rate can be absorbed by the coolant. More detailed calculations needed for a specific optimized design, but this simple estimate shows that the heat exchange capability of such device is not small at all. Depending on the target and beam required for an application, or class of applications, the parameters of the device such as dimensions, choice of materials, number and thickness of the radiating fins, can be selected.

## Rotating target for the GDNP experiment

The **Rotating Target** device can be used in the GDNP experiment, to avoid local overheating and melting of the gold target. I would propose using Au/Cu combination of target/absorber. The heat sink can be made of copper, or tungsten. Copper melts at 1357K, has Thermoconductivity 4.01 [W/cm/K], and also can be fused with gold to produce ideal thermal contact. The rotating target solution for the Au/Cu combination looks OK, at a first glance, assuming that the hot parts are made of Cu. The volume and the effective cooling surface of the beam spot can easily be made, respectively, 300 and 100 times larger than for a local "hot spot" (assuming the diameter of the ring is 10cm). I would expect that the equilibrium temperature of the hot radiator could be kept at 700-800K, to give some room for instant heating by the beam. The number of radiative heat exchange fins can be kept reasonable (I would guess between 20 and 60). The induction coils can be used to rotate the hot assembly with high speed.

Final design would require detailed calculations and optimization in the choice of materials and geometry.

Figure 1. Electron beam interactions in 0.75-mm Au target mounted on 1-cm Al plate. E = 8 MeV, $\sigma_x \times \sigma_y = 0.5 \times 0.5$ mm. 100 interactions modeled by GEANT.

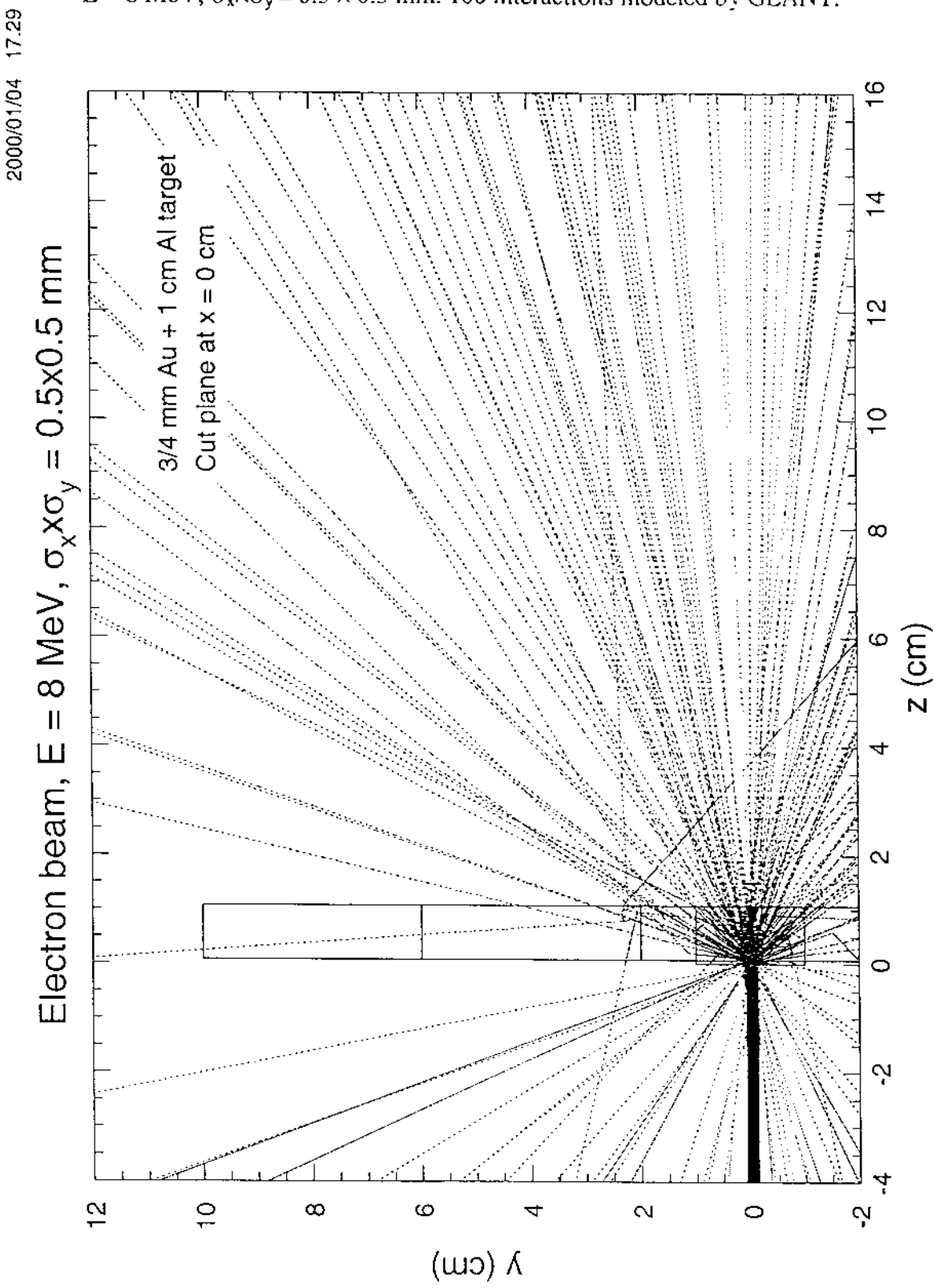

Figure 2. Power density distribution in Au / Al target as a function of longitudinal coordinate along beam, at different radial distances from z-axis.

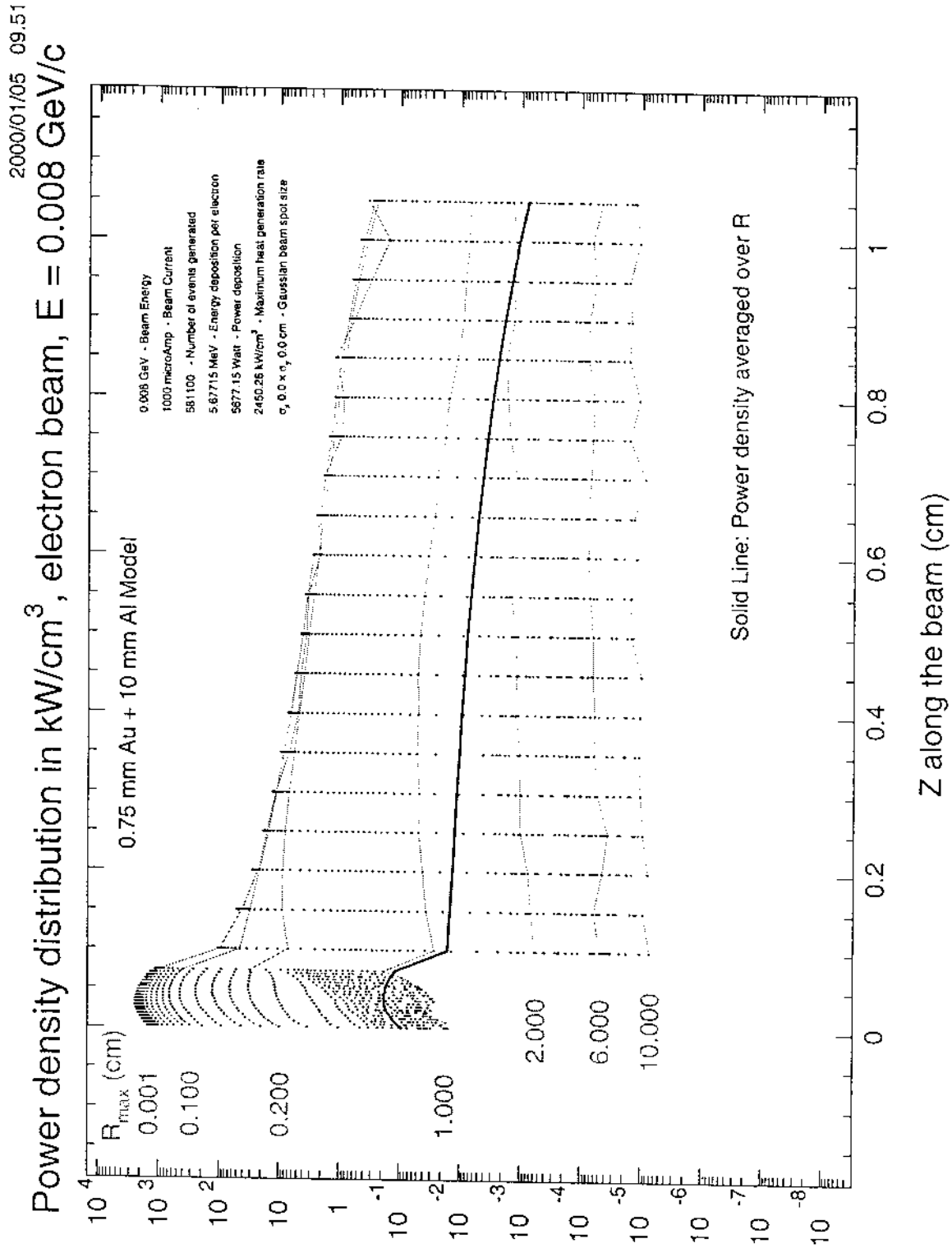

Figure 3. Equilibrium temperature distribution in the 0.75-mm thick gold plate assuming that the plate's back surface is kept at room temperature. The temperatures are shown as color(density)-mapped with the scale in K shown in the insert.

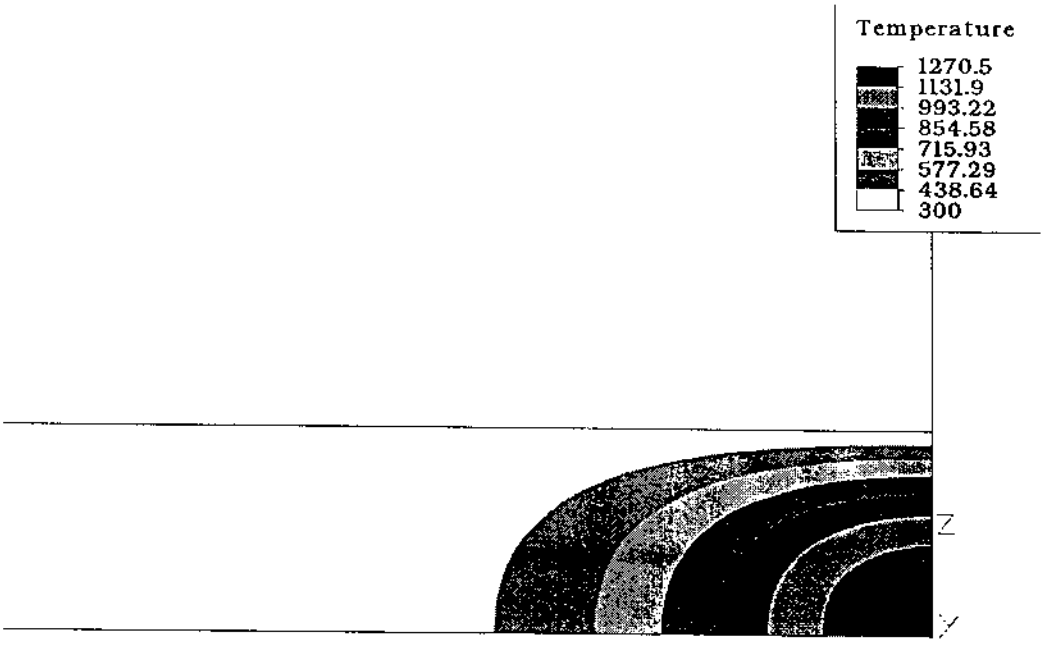

Figure 4. Schematic design of the Rotating Target Device.

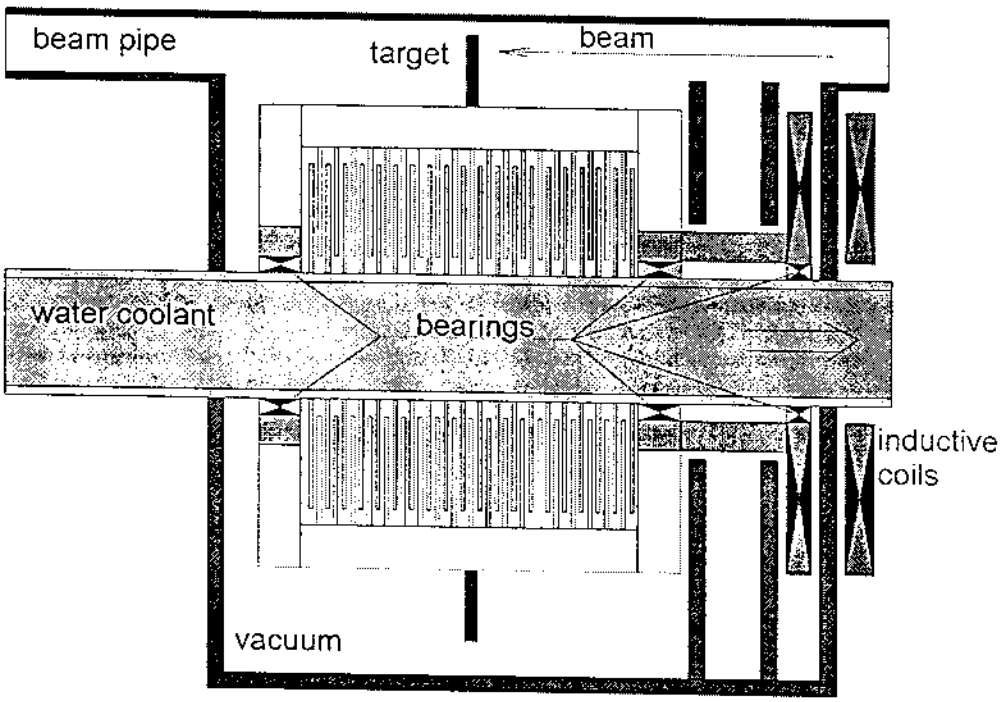

# Measurement of parity violation in the photodisintegration of deuterium and in the production of bremsstrahlung on tantalum

E. D. EARLE, A. B. MCDONALD,[1] S. H. KIDNER, E. T. H. CLIFFORD,[2] J. J. HILL, AND G. H. KEECH
*Chalk River Nuclear Laboratories, Chalk River, Ont., Canada K0J 1J0*

AND

T. E. CHUPP[3] AND M. B. SCHNEIDER[4]
*Physics Department, Princeton University, Princeton, NJ 08544, U.S.A.*

Received May 28, 1987

The circular polarization dependent component of the total cross section for photodisintegration of deuterium has been measured: $(2.7 \pm 2.8) \times 10^{-6}$ for bremsstrahlung with an end point of 4.1 MeV and $(7.7 \pm 5.3) \times 10^{-6}$ for an end point of 3.2 MeV. The helicity-dependent component of the total cross section for the production of bremsstrahlung on tantalum by longitudinally polarized electrons has been measured: $(0.63 \pm 0.70) \times 10^{-6}$ for an electron energy of 4.1 MeV and $(3.1 \pm 1.5) \times 10^{-6}$ at 3.2 MeV. All measurements are in agreement with theoretical predictions for these processes.

Les valeurs de la composante de la section efficace totale de photodésintégration du deutérium qui dépendent de la polarisation circulaire mesurée avec faisceau de radiation de freinage allant jusqu'à 4,1 et 3,2 MeV respectivement, sont de $(2,7 \pm 2,8) \times 10^{-6}$ et $(7,7 \pm 5,3) \times 10^{-6}$. La composante de la section efficace totale pour la production de radiation de freinage sur le tantale par des électrons polarisés longitudinalement a été évalué à $(0,63 \pm 0,70) \times 10^{-6}$ pour des électrons de 4,1 MeV et $(3,1 \pm 1,5) \times 10^{-6}$ à 3,2 MeV. Toutes les mesures sont en accord avec les prédictions théoriques pour ces processus.

[Traduit par la revue]

Can. J. Phys. 66, 534 (1988)

## 1. Introduction

Measurements of parity violation in light nuclear systems have been pursued for many years with the objective of defin[illegible] weak nucleon–nucleon interaction as completely as possible. These experiments have been performed on basic two-nucleon systems (1–4) and also on more complex nuclei (for a summary, see ref. 5), with the emphasis on those nuclei where parity-violation effects are enhanced and whose nuclear structure is well understood. In addition, theoretical calculations have been performed extensively. Significant progress has been made (6) through the inclusion of the Glashow–Weinberg–Salam (GWS) Standard Model with quark models of the nucleon, and acceptable ranges of parameters for the weak nucleon–nucleon interaction have been defined.

Parity-violation measurements in the two-nucleon system have been performed previously in only three cases. Measurements have been made of the scattering of polarized protons from hydrogen at several energies (1), with statistically significant results in agreement with theory. The parity-violating component in the scattering cross section was found to be about $2 \times 10^{-7}$. Measurements have also been made for the parity-violating asymmetry in gamma-ray emission following the capture of polarized cold neutrons. The most recent result (2) has been $A = (-5 \pm 5) = 10^{-8}$, to be compared with a theoretical prediction of $0.2 = 10^{-7}$. One of the first measurements in the two-nucleon system was performed by Lobashov *et al.* (3), who measured the circular polarization of gamma rays produced in the capture of thermal neutrons in hydrogen. They obtained a value of $(-1.30 \pm 0.45) \times 10^{-6}$, in disagreement with many theoretical calculations predicting a value less than $0.5 \times 10^{-8}$. Recent measurements (4) by the same group have uncovered problems in the original work and defined an upper limit of $0.5 \times 10^{-7}$ for the circular polarization.

We have performed a measurement of the inverse reaction [D(γ,n)p] and measured the helicity dependence in the cross section for the photodisintegration of deuterium by circularly polarized gamma rays. Near threshold, this reaction is sensitive to the same components of the weak nucleon–nucleon interaction as the thermal neutron capture, but at higher energies it is sensitive to additional components. For all energies within 2 MeV above threshold, the helicity-dependent part of the cross section is calculated (7, 8) to be less than $5 \times 10^{-8}$ of the total cross section. We have also performed a sensitive measurement of the change in intensity of bremsstrahlung produced by beams of polarized electrons striking tantalum at energies of 3.2 and 4.1 MeV. This is the first search for parity violation in this process. Extrapolations of the calculations of Kerimov and Safin (9) indicate that effects smaller than about $1 \times 10^{-9}$ are expected from the GWS Standard Model at these energies.[5]

## 2. Experiment

A schematic diagram of the experiment is presented in Fig. 1. Polarized electrons are generated in a gallium arsenide photoemission source modelled on the Peggy II source at the Stanford Linear Accelerator Center (SLAC) (10), and are accelerated in the Electron Test Accelerator (ETA) at Chalk River Nuclear Laboratories. Electrons at energies of 3.2 or 4.1 MeV strike a water-cooled tantalum radiator, producing bremsstrahlung for which the highest energy gammas have a circular polarization nearly equal to the longitudinal polarization of the electrons, about 35%. The bremsstrahlungs strike a 0.2 cm$^3$ $D_2O$ target and generate neutrons, which are thermalized by

[1]Present address: Physics Department, Princeton University, Princeton, NJ 08544, U.S.A.

[2]Present address: TRIUMF, University of British Columbia, Vancouver, B.C., Canada V6T 1W5.

[3]Present address: Physics Department, Harvard University, Cambridge, MA 02138, U.S.A.

[4]Present address: Physics Department, Grinnel College, Grinnel, IA 50112, U.S.A.

[5]Also M. Y. Safin, private communication.

Printed in Canada / Imprimé au Canada

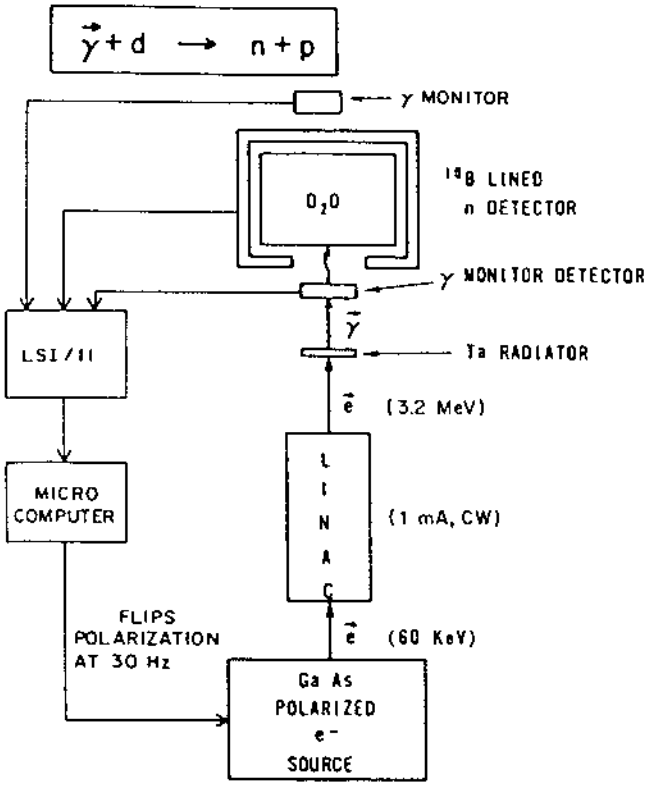


FIG. 1. Schematic diagram of the experiment.

the $D_2O$ and detected in boron-lined, high-efficiency neutron detectors. The photodisintegration measurement searches for a change in total neutron intensity correlated with the reversal of the gamma-ray circular polarization. To observe any change in gamma-ray intensity upon reversal of the electron helicity, we have mounted a large-area, gamma-sensitive detector directly on the bremsstrahlung radiator.

The main difficulty in searching for small parity-violating effects correlated with polarization reversal is ensuring that the observed intensity changes have not been induced by some other systematic effect unrelated to the change in electron polarization. Therefore, many pieces of subsidiary equipment were employed to monitor a wide variety of parameters, which could change when the electron polarization is reversed and induce a gamma-ray or neutron intensity change. These parameters were artificially varied with large amplitude during a series of measurements, and the sensitivity of the monitors was determined. At the same time, the sensitivity of the total gamma-ray intensity and the total neutron intensity to these parameters was determined. In this way, by observing these monitors during the extended running time used to measure parity violation, we were able to determine corrections to the gamma-ray and neutron intensity arising from effects other than parity violation.

The polarized-electron source design was nearly identical to Peggy II (10); an internal cryopump was added to make pressures of less than $1 \times 10^{-10}$ Torr easier to obtain (1 Torr = 133 Pa). Polarized electrons were emitted from a p-type GaAs crystal, doped with $1 \times 10^{-19}$ Zn atoms/cm$^3$, cleaved in the 100 direction, mechanically polished, and coated with a few monolayers of cesium and oxygen. The crystals were chemically cleaned, anodized, and then etched immediately before installation in the vacuum system to ensure surface cleanliness. Circularly polarized laser light was obtained from a Kr-ion laser, which provided a continuous beam of up to 1.5 W of 752 nm light. The circular polarization was produced by a high-quality linear-polarizing prism, followed by a Pockels cell acting as a quarter-wave plate. The circular polarization could be rapidly reversed by reversing the 2600 V bias on the Pockels cell. This reversal produced a corresponding reversal of the longitudinal polarization of the electron beam with a fractional change of less than $7 \times 10^{-5}$ in electron-beam intensity. The GaAs crystals were cleaned in place by heating with an electron gun in a separate vacuum chamber behind the crystal mounting plate. After cleaning and activation with cesium and oxygen, they provided a stable beam current between 350 and 700 μA for 1.2 W of laser light. This was accelerated with about 70% transmission efficiency to the target. Source emission typically had a half-life of a few hours but could be returned to near the original level by the addition of a small amount of cesium and oxygen.

Figure 2 gives a more complete schematic representation of the experiment, showing the polarized source, accelerator, and experiment area. The polarized electrons were accelerated to 3.2 or 4.1 MeV and struck a 0.04 cm thick tantalum bremsstrahlung radiator, backed by a 1 cm thick stream of flowing water for cooling. The use of a thin tantalum radiator maximized the bremsstrahlung production above the photodisintegration threshold. To reduce the energy density, we had the beam rapidly swept vertically (300 Hz) and horizontally (360 Hz) by sinusoidal signals applied to a pair of deflection coils, creating a 10 cm$^2$ beam spot on the tantalum. The bremsstrahlung radiator was reentrant 18 cm into a $D_2O$ target can 0.6 m long and 0.5 m$^2$. The geometry of the can was chosen through Monte Carlo calculations to provide a compromise between efficient thermalization for capture of neutrons in the B detectors and minimal scattering time in $D_2O$, enabling fast helicity switching. About 60% of the neutrons produced by bremsstrahlung above the 2.2 MeV threshold were thermalized, and about 90% of these had left the $D_2O$ volume within 2 ms. Electron currents could be measured from the tantalum radiator and from a large aperture obscuring all beam trajectories outside the tantalum plate.

Electron polarization was measured by Mott scattering from gold foils at 60 keV in an off-line apparatus. These measurements indicated polarizations of about 35% under typical operating conditions. The gamma-ray polarization was determined several times during the experiment by measuring the circular polarization of the bremsstrahlung at the target end of the accelerator. For these measurements, the bremsstrahlung passed through a 10 cm long, iron transmission polarimeter (developed for a measurement of parity violation in $^{21}$Ne (11)) and was detected in a 3 cm$^3$ intrinsic germanium detector. The circular polarization as a function of gamma-ray energy was inferred from the known detector response function and polarimeter efficiency. Near the tip of the bremsstrahlung spectrum, the measured gamma-ray circular polarization was 30%.

Five sides of the $D_2O$ target were covered with a total of 20 neutron detectors developed at Chalk River for the experiment.[6] These detectors contained two regions of hydrogen-filled ionization chambers. The first region contained nine zircalloy plates, 0.25 mm thick, coated on two sides with about 0.3 mg/cm$^3$ of boron to detect neutrons via the $^{10}B(n,\alpha)^7Li$ reaction. The second region contained six similar plates without boron coating and was used to determine the gamma-ray

[6] E. D. Earle et al. [illegible]

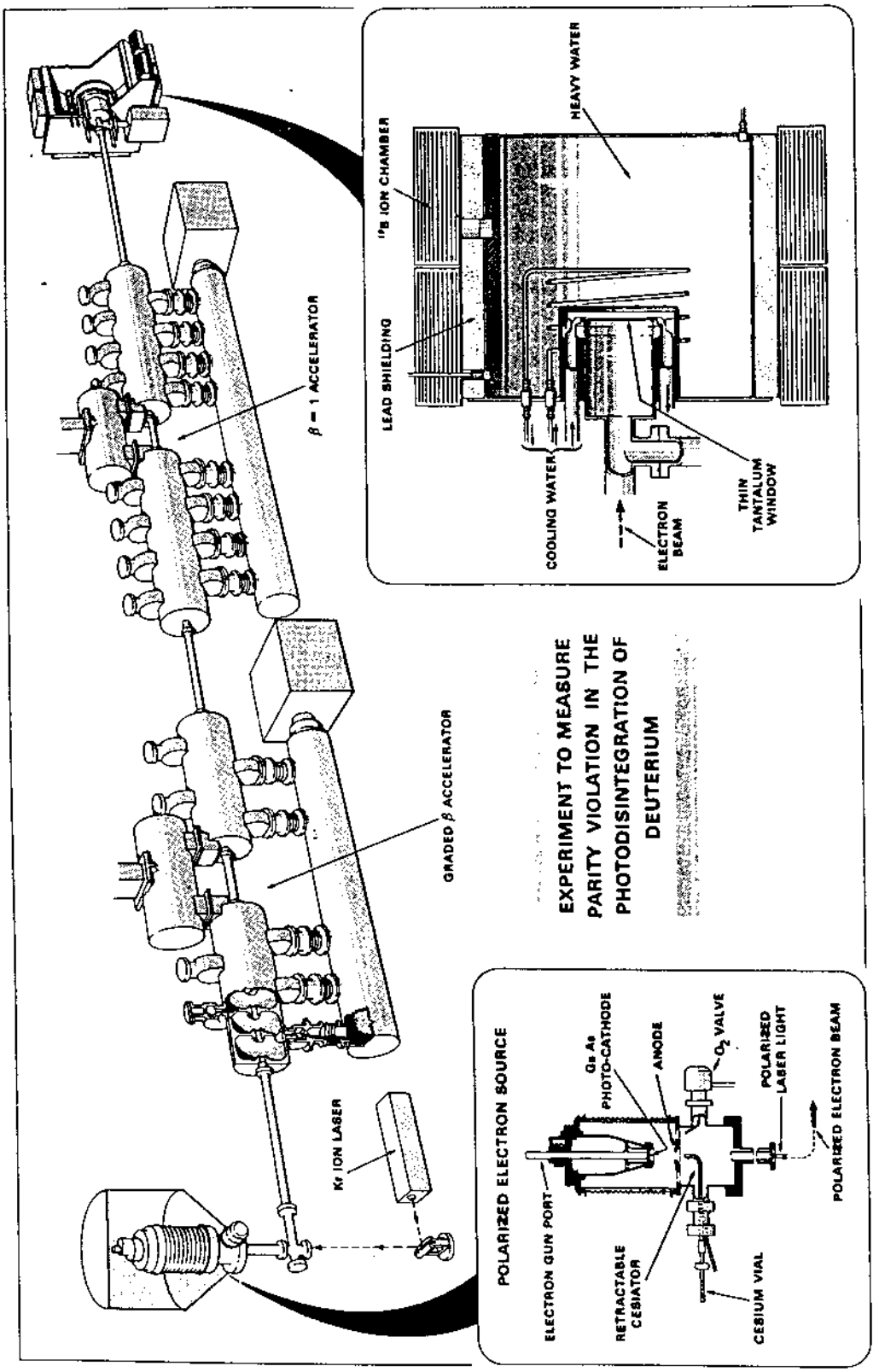


FIG. 2. Schematic drawing of the experimental apparatus.

contribution to t
ness was chose
lithium and heli
mize the neutro
boron was such
the detectors we
sure was 1 atm (
ated at 300 V bi
tion of thermal n
background. Th
about 3 × 10⁻¹
tions produced
this meant that
section of the d
the boron. These
ionization cham

For experime
necessary to me
vidual pulses. T
rents to frequen
CAMAC-based
processor gener
reversal of the e
the beam on–o
symmetrized to
had a frequency
erator noise. Sh
processor and s
electron source
counting room c
city reversal. Th
measure the zer

The main par
the neutron and
intensity, energ
there is a change
reversal of the
effect on the ove
parameters varie
the measuremen
experimental are

The electron-
the current from
very good Farad
the beam strikin
ray detectors di
modelled on "se
(12). They consi
tor made of tung
In the intense ga
10 pA was produ
in these two ma
thick and 13 cm
of 1.4 cm. Half
half, vertically.
the centroid and
the radiator. We
currents from the
which produced
first and second
each direction.
from the BIC d

contribution to the current in the first section. The boron thickness was chosen to optimize the efficiency for escape of the lithium and helium ions into the hydrogen gas and also maximize the neutron-detection efficiency. The total thickness of boron was such that 90% of the thermal neutrons incident on the detectors were captured in the boron. The hydrogen pressure was 1 atm (1 atm = 101 kPa), and the detectors were operated at 300 V bias. This design worked very well for the detection of thermal neutrons in the presence of an intense gamma-ray background. The neutron sections of the detector produced about $3 \times 10^{-13}\,\mathrm{A \cdot neutron^{-1} \cdot cm^{-2} \cdot s^{-1}}$, and the gamma sections produced about $1 \times 10^{-14}\,\mathrm{A \cdot rad^{-1} \cdot s^{-1}}$. At 4.1 MeV, this meant that about 90% of the current in the boron-coated section of the detector was due to thermal neutron capture in the boron. These detectors will be referred to as the BIC (boron ionization chambers) in further discussion.

For experimental sensitivities better than $1 \times 10^{-6}$, it was necessary to measure currents from detectors, rather than individual pulses. The electronic system converted detector currents to frequencies of about 5 MHz, which were scaled with a CAMAC-based LSI-11 acquisition system. A separate microprocessor generated a switching pattern, which controlled the reversal of the electron helicity, the data-acquisition times, and the beam on–off times. The helicity reversing pattern was symmetrized to compensate for long-term intensity drifts and had a frequency of about 30 Hz, as required to minimize accelerator noise. Short transient pulses were generated by the microprocessor and square waves were synthesized at the polarized electron source for polarization reversal to avoid pickup in the counting room of the square-wave signals correlated with helicity reversal. The beam was turned off for 4 s in every 100 s to measure the zero levels of all detector systems.

The main parameters expected to cause systematic effects in the neutron and gamma-ray intensities are the electron-beam intensity, energy, position, and size. Problems can arise if there is a change in any of these parameters correlated with the reversal of the electron polarization. There can also be an effect on the overall accuracy of the experiment if any of these parameters varies randomly and introduces excessive noise in the measurement. Figure 3 shows a schematic diagram of the experimental area with systematic monitoring devices in place.

The electron-beam intensity was monitored by measuring the current from the bremsstrahlung radiator, which served as a very good Faraday cup. To determine the position and size of the beam striking the radiator, we mounted an array of gamma-ray detectors directly on the radiator. These detectors were modelled on "self-powered" detectors used for reactor control (12). They consisted of coaxial cables with the central conductor made of tungsten and the outer shield made of aluminum. In the intense gamma-ray fluxes used, a current in the order of 10 pA was produced from the difference in Compton scattering in these two materials. An array of sixteen detectors, 0.3 cm thick and 13 cm long, was used with an interdetector spacing of 1.4 cm. Half of them were aligned horizontally; the other half, vertically. This array was very effective in determining the centroid and width of the gamma-ray distribution leaving the radiator. We extracted this information by amplifying the currents from the detectors and sending this to analog circuitry, which produced signals proportional to the total current and the first and second moments of the gamma-ray distribution in each direction. Additional position information was obtained from the BIC detectors, which provided total current signals

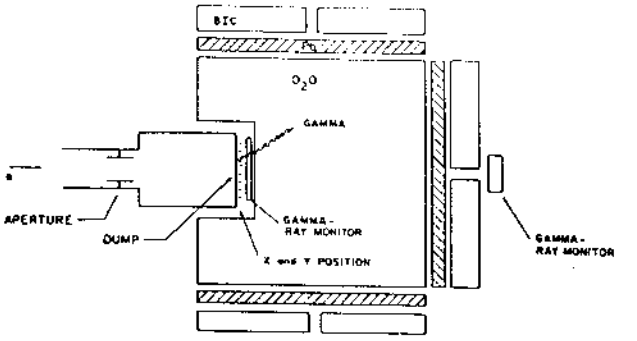


FIG. 3. More detailed diagram of the target region. The BIC are used to detect thermal neutrons.

from the neutron and gamma-ray sensitive regions for the set of detectors on the top, bottom, left, right, and end of the $D_2O$ tank.

As mentioned above, a large-area gamma detector was mounted directly on the radiator to determine the total gamma-ray flux produced for each helicity. This detector also produced a current from the difference in Compton scattering from dissimilar materials. It consisted of 14.3 cm diameter plates of aluminum and lead, 0.3 mm thick. This configuration produced about 100 pC/rad, and therefore the detector provided currents of nA in the actual operation on the bremsstrahlung radiator. It is referred to as the PPSPD (parallel plate self-powered detector). To determine the energy variation of the electron beam upon helicity reversal, we mounted a small-volume (10 $\mathrm{cm^3}$) bismuth germanate detector (BGO) on the end of the $D_2O$ tank at 0°. The variation of the bremsstrahlung angular distribution and attenuation with energy produced an energy dependence in the current from this detector when compared with the total bremsstrahlung flux measured by the PPSPD.

## 3. Data acquisition

The monitors were calibrated at 3.1 and 4.2 MeV in a series of measurements (referred to as modulation data), wherein the electron-beam intensity, energy, position, and size were modulated with the same switching pattern used for the reversal of the electron helicity in the main measurement. These data were used to determine the sensitivity of all detectors to these parameters. By modulating these parameters with a pattern similar to the electron helicity switching, we could use these measurements to appropriately determine the effects of detector response time.

Data taking for the determination of parity violation then proceeded, and the monitor detectors were used to measure the variation of the above electron beam and gamma-ray flux parameters during the measurement.

By a 90° rotation of the plane of polarization of the incident laser light prior to the Pockels cell, it was possible to reverse the circular polarization of the photoemission light for a given voltage applied to the Pockels cell. Therefore, the overall sense of the electron polarization could be changed relative to the electronic switching patterns. About one half of the parity-violation data was taken with each overall sense of the electron polarization. True parity-violation effects must be correlated with this overall polarization reversal and can be sought as the difference between helicity-correlated quantities determined for the two overall senses of the electron polarization. On the other hand, systematic effects correlated only with the electronic

TABLE 1. Fractional changes correlated with parameter modulation (units of $10^{-6}$); beam energy = 4.1 MeV

| du/ ram. | Beam | BIC ($N$) | PPSP ($\gamma$) | BGO ($\gamma$) | $N_X$ | $N_Y$ | $X_{POS}$ | $Y_{POS}$ | $X_{WID}$ | $Y_{WID}$ |
|---|---|---|---|---|---|---|---|---|---|---|
| ensity | 5025 | −14 | 135 | −97 | −2 | 23 | 69 | −46 | −66 | 16 |
| ergy | 58 | 2323 | 603 | 1781 | −67 | 49 | −186 | −14 | −77 | −64 |
| position | 13 | −36 | −46 | 4 | −1213 | 9 | −3520 | −112 | −81 | 42 |
| position | 11 | 32 | 10 | −431 | −120 | −1218 | −237 | 3672 | −93 | 9 |
| size | 28 | −14 | 384 | −156 | 11 | 89 | 5 | 3 | 117 | −1534 |

itching pattern are the same for each orientation of the prism l cancel if differences are calculated between the two orien- ons.

n addition, by a 45° rotation of the plane of polarization of incident laser light, it was possible to produce very small gitudinal polarization for the electron beam. Some data were ɔ taken under this condition.

## 4. Data analysis

### '. General

Scaler values proportional to the currents in the various ectors, integrated over the period corresponding to one sense he electron helicity, were the primary data for the measure- nt. Seventeen scalers were used: 10 corresponding to cur- ts from the neutron and gamma sections of the BIC detectors the four sides and end of the $D_2O$ tank; three corresponding the total current and the first and second moments of the nma-ray flux striking the self-powered detector array on the ms- lung radiator; and one each for the beam current on ra r, the beam-defining aperture, the PPSPD, and the O detector.

The on-line analysis program in the CAMAC crate-based I-11 computer wrote this data on magnetic tape in buffers responding to 16 sets of scalar readings, together with infor- tion about whether the symmetric helicity switching pattern gan with a positive or negative helicity state. For all detectors l monitors, quantities of the form $A = (D_+ - D_-)/(D_+ + D_-)$ re derived, where $D_+$ ($D_-$) represents the average current asured in a detector when the state of the electronic switch- ; pattern was plus (minus). In addition, the on-line program s capable of calculating averages and variances for these icity-correlated quantities, but it was only fast enough to ndle one seventh of the data. Therefore, it was possible to serve parity-violation signals, systematic monitoring signals, d their variances on-line with restricted accuracy, but a com- te data analysis had to wait for playback of the magnetic es with a more complete program on the Chalk River central mputer system. The final data-analysis program also incorp- ated the ability to correct individual parameters on a buffer- -buffer basis and to produce correlation plots and linear gressions on selected parameters.

### 2. Modulation data

The relative magnitudes of the various systematic effects re determined from the modulation data. When the overall am intensity was modulated, it was found that all detectors owed similar fractional changes in counting rate, indicating ce linearity and similar response time. Residual correc- ns were a few percent of the modulation amplitude in most ses. Therefore, before further analysis, the scaler value for ch detector was divided by the value obtained from the cur- nt measured on the bremsstrahlung radiator. This compensa- tion for rapid beam-current fluctuations greatly reduced the variance of all detector signals. From here on, the discussion is given in terms of such beam-corrected signals.

Table 1 shows the sensitivity of various quantities to modulations of beam intensity, energy, position, and size. Beam intensity was modulated by varying the intensity of the incident laser light. Beam energy was modulated by varying the rf power to one of the acceleration cavities. Beam position and size, respectively, were modulated by varying the dc offset or amplitude of the function generators producing the high-frequency sweeping of the beam on target. In all cases, the time sequence of the modulation was similar to the helicity reversal pattern used in the accumulation of parity-violation data. The BIC, PPSPD, and BGO quantities given in the table incorporate a linear correction for beam intensity, as described above.

Typical uncertainties in tabulated quantities are less than $10^{-5}$, as determined from variances in the observed values.

The quantities $X_{POS}$, $Y_{POS}$, $X_{WID}$, and $Y_{WID}$ were obtained from the position-sensitive array of self-powered detectors, corresponding to the first and second moments of the bremsstrahlung angular distribution at the target. The quantities $N_X$ and $N_Y$ were calculated from the signals obtained from the BIC neutron detector array.

For example, $N_X$ is

$$N_X = [N(\text{left}) - N(\text{right})]/[N(\text{left}) + N(\text{right})]$$

A similar formula is used for the vertical difference $N_Y$. As can be seen from Table 1, these quantities are a sensitive measure of beam motion on target through the associated motion of the neutron flux striking the BIC detectors.

A discussion of the modulation data in Table 1 will illustrate the sensitivity of the various detectors to systematic variation of beam parameters, correlated with electron helicity reversal.

First, the intensity modulation data illustrate that normalization by beam division is very effective in reducing the sensitivity to beam intensity. The residual sensitivity in the sum of the neutron detectors divided by beam current is particularly small (less than $3 \times 10^{-3}$), implying very little overall effect when coupled with beam-intensity fractional changes of less than $7 \times 10^{-5}$ during the recording of parity-violation data.

The modulation of energy revealed that the total neutron flux shows the largest sensitivity to beam-energy variations. The total gamma-ray flux, as measured by the PPSPD, only varied about 0.25 times as much. This was because of the variation of the photodisintegration cross section with energy, which enhances the neutron-flux sensitivity. However, the BGO detector, observing only gamma rays at 0°, showed a fractional variation about 0.7 times that of the BIC neutron detectors. The enhanced energy sensitivity was due to changes in the bremsstrahlung angular distribution and differential absorption of the gamma rays at 0°. This detector therefore constituted our

primary energy n
gamma-flux (PPS
for systematic be
The beam posi
lent sensitivity of
strahlung radiato
in extracting the
on target is also e
of the beam cen
about 1 cm of dis
is very effective i
tion, for motion i
response in the 1
the beam width
very little spuriou
signals, $X_{POS}$ an
In addition, it i
tion data that the
of the centroids c
On the other han
insensitive to mo
distribution or ch
the responses of
tion data, it is cle
fractional change
line between the
expected, but th
experiment with
the wide beam d
distribution, and
The care taken t
the BIC detector
ring here.
Two additiona
position and siz
exhibits a small
size, due to its
exhibits a small s
tivities are small
rections because
observed for the

### 4.3. Parity-viola

Having determ
function sensitive
tween them, we
with electron hel
effects. These ac
magnitude of the
tion, and size cor
During the acc
observed that the
ited clear correla
with slopes corr
correlated beam-e
or -size monitors
the above three
effects observed
cluded that the lar
correlated beam-
the total neutron
$1 \times 10^{-6}$, respec
Therefore, the

primary energy monitor and could be used to correct the total gamma-flux (PPSPD) and total neutron-flux (BIC $N$) signals for systematic beam-energy variations.

The beam position and size modulations illustrate the excellent sensitivity of the self-powered detector arrays on the bremsstrahlung radiator. The effectiveness of the electronic circuitry in extracting the first and second moments of the beam shape on target is also evident in the data. The actual $X$ and $Y$ motions of the beam centroid for the data in Table 1 correspond to about 1 cm of displacement, so it is clear that the detector array is very effective in the measurement of beam motion. In addition, for motion in the $X$ direction, there is very little spurious response in the $Y$ detectors and very little response in $X_{\mathrm{WID}}$, the beam width signal. For the modulation of $Y$-beam size, very little spurious response is observed in the $X$- and $Y$-position signals, $X_{\mathrm{POS}}$ and $Y_{\mathrm{POS}}$.

In addition, it is apparent from the position and size modulation data that the $N_X$ and $N_Y$ signals are also sensitive indicators of the centroids of the neutron flux striking the BIC detectors. On the other hand, the sum of all the neutron detectors is very insensitive to movements of the centroid of the neutron-flux distribution or changes in its shape. From an examination of the responses of individual neutron detectors to these modulation data, it is clear that opposite detectors exhibit very similar fractional changes when the beam centroid is moved along a line between them. To first order in beam position, this is expected, but the cancellation is even more effective in this experiment with such a diffuse neutron-flux shape caused by the wide beam distribution on target, the gamma-ray angular distribution, and the thermalization process for the neutrons. The care taken to obtain very similar neutron efficiencies for the BIC detectors is also rewarded by the cancellations occurring here.

Two additional sensitivities are also important to note in the position and size modulation data. First, the BGO detector exhibits a small sensitivity to $Y$-position modulation and $Y$ size, due to its asymmetric shape. In addition, the PPSPD exhibits a small sensitivity to beam size. In fact, the size sensitivities are small enough that they have little influence as corrections because of the very small values of $X_{\mathrm{WID}}$ and $Y_{\mathrm{WID}}$ observed for the parity-violation data.

### 4.3. *Parity-violation data*

Having determined that the various monitors performed their function sensitively, with relatively little cross correlation between them, we were able to accumulate parity-violation data with electron helicity reversing and with minimal systematic effects. These active monitors then served to determine the magnitude of the variations in beam intensity, energy, position, and size correlated with helicity reversal.

During the accumulation of the parity-violation data, it was observed that the PPSPD and the BGO detector signals exhibited clear correlations with the neutron signals from the BIC, with slopes corresponding to those expected for a helicity-correlated beam-energy modulation. None of the beam-position or -size monitors showed significant correlations with any of the above three primary signals, as expected from the small effects observed in the modulation data. It was therefore concluded that the largest remaining systematic effect was a helicity-correlated beam-energy variation, producing contributions to the total neutron and gamma-ray signals of about $3 \times 10^{-6}$ and $1 \times 10^{-6}$, respectively.

Therefore, the corrections for systematic effects in the parity-violation data were carried out as follows. First, the signals obtained from the neutron sections of the BIC detectors were corrected for the small gamma component in the signal by subtracting a fraction of the signal in the gamma sections of each detector. (The relative sensitivity to gamma rays was determined from runs where $H_2O$ replace $D_2O$.) Then, the signals from all detectors and monitors were divided by the signals obtained for the beam current on the bremsstrahlung radiator. The helicity-correlated values, "$A$", were then calculated for all signals. The BIC, PPSPD, and BGO $A$ values were then corrected slightly for small ($<10^{-6}$) beam position, size, and residual intensity effects, using the sensitivities measured from the modulation data. Finally, the sum of the BIC neutron detectors and the PPSPD were corrected for residual beam energy-variation, using the BGO values as a monitor of this quantity.

Table 2 shows the results at 4.1 MeV electron energy for various stages of the analysis. The overall helicity values, plus, minus, and zero, correspond to values of the prism in the light path providing electrons with plus, minus, or zero helicity for the positive state of the switching pattern. The BIC $N$ values correspond to the sum of all BIC neutron sections and therefore are a measure of the fractional change in total neutron flux upon helicity reversal. The PPSPD values indicate the fractional change in total bremsstrahlung flux. The numbers in parentheses indicate one standard deviation as derived from the average variance of the quantity evaluated for individual buffers. Note that the standard deviation for the BIC $N$ values is reduced at each stage of the correction process as the influence of fluctuations in intensity and beam energy are removed.

The standard deviations in the table represent only the residual fluctuations in the quantities after the corrections have been applied. However, additional uncertainties arise because the correction factors determined from the modulation data have inherent uncertainties in the order of 15%. For example, the complete formula for correction of the BIC $N$ results is

$$A(\mathrm{BIC}\,N) = A(\mathrm{BIC}\,N/\mathrm{BEAM}) - 0.027A(\mathrm{BEAM}) - 1.39A^{\mathrm{I}}(\mathrm{BGO/BEAM})$$

where

$$A^{\mathrm{I}}(\mathrm{BGO/BEAM}) = A(\mathrm{BGO/BEAM}) - 0.35A(N_Y) + 0.04A(\mathrm{BEAM})$$

Corrections for other beam-size and -position effects are negligible. Although all quantities other than beam intensity exhibit $A$ values less than $\approx 4 \times 10^{-6}$, uncertainties of 15% in the coefficients increase the final uncertainty significantly. The final columns in Table 2 indicate the overall uncertainties, which are dominated in most cases by uncertainties in the corrections.

Final values of the parity-violating observables are

$$A_{PV}(\mathrm{NEUTRON}) = [A_+(\mathrm{BIC}\,N) - A_-(\mathrm{BIC}\,N)]/2$$

$$A_{PV}(\mathrm{GAMMA}) = [A_+(\mathrm{PPSPD}) - A_-(\mathrm{PPSPD})]/2$$

where + (−) refers to the overall helicity value. These asymmetries must be divided by the average gamma-ray or electron polarization to determine the final cross-section asymmetry. These polarizations are taken to be $0.30 \pm 0.05$, as determined by the measurements of bremsstrahlung circular polarization.

Table 3 lists the final results at the two energies studied. The results at 3.2 MeV are less accurate because of lower yields,

TABLE 2. Helicity correlated asymmetry values (units of $10^{-6}$); 4.1 MeV data

| :ra city sm) | BIC $N$ (uncorrected) | Beam current | BIC $N^a$ (divided) | PPSPD$^a$ (divided) | BGO$^a$ (divided) | BIC $N^b$ (corrected) | PPSPD$^b$ (corrected) | BIC $N^c$ (inclusive) | PPSPD$^c$ (inclusive) |
|---|---|---|---|---|---|---|---|---|---|
| ıs | 72.2 (±0.9) | 70.0 (±0.7) | 2.2 (±0.46) | 3.0 (±0.18) | 1.1 (±0.35) | −1.4 (±0.3) | 0.69 (±0.14) | −1.4 (±1.6) | 0.69 (±0.38) |
| nus | 1.1 (±1.0) | 4.2 (±0.7) | −3.1 (±0.56) | 0.39 (±0.22) | −2.8 (±0.40) | 0.30 (±0.3) | 0.31 (±0.14) | 0.30 (±0.60) | 0.31 (±0.17) |
| ro | −117.8 (±1.6) | −115.0 (±1.3) | −2.8 (±1.2) | −3.9 (±0.54) | 1.4 (±0.95) | −0.77 (±1.0) | −0.50 (±0.90) | −0.77 (±1.8) | −0.50 (±1.7) |

Divided by beam current.
Corrected for beam current, energy, and size.
Includes uncertainties in corrections.

TABLE 3. Parity-violating observables (units of $10^{-6}$)

| eam ergy | Quantity observed | Measured asymmetry | Cross-section asymmetry |
|---|---|---|---|
| MeV | Neutrons | 0.85±0.86 | 2.7 ±2.8 |
| | Gammas | 0.19±0.21 | 0.63±0.70 |
| MeV | Neutrons | 2.3 ±1.6 | 7.7 ±5.3 |
| | Gammas | 0.94±0.46 | 3.1 ±1.5 |

ıpled with less running time and lower intensity caused by er culties near the end of the running period. Subse- en his running period, the ETA facility was shut down, cluding further measurements.

As can be seen from Table 2, final uncertainties were domi- ed by uncertainties in the corrections made for systematic ects. As judged by the residual fluctuations in the BIC $N$ and SPD values, the accuracy of the final result could be about o to three times better if systematic changes in beam inten- y and energy were reduced. In fact, measurements of ther- l neutron fluxes by the activation of gold foils indicated that residual fluctuations in the neutron detector signals were ly about 1.4 times the ideal statistical value of (number of atrons detected)$^{-1/2}$.

## 5. Conclusions

None of the results in Table 3 exhibit a statistically signifi- ıt parity-violating effect. The results for photodisintegration $D_2O$ are in agreement with theoretical calculations (7, 8) ıt indicate that expected effects are less than about $5 \times 10^{-8}$ these energies. The calculations of Oka (8) show that at 2 MeV, the photodisintegration measurement is expected to dominated by weak $\pi$ exchange terms. At threshold, both lculations (7, 8) indicate that $\pi$ exchange terms are small, so parity-violation effects are dominated by weak $\rho$ and $\omega$ change. The present measurements and the measurements of the p(n,$\gamma$)d inverse reaction at threshold have not reached level of sensitivity necessary to define parameters of the eak nucleon–nucleon interaction. However, the removal of r discrepancy with theory presented by the original measurements (3) means that essentially all measure- ents of parity-violation effects in two-nucleon and light nuclear stems are consistent with theory (5).

The present experiment is the first measurement of parity olation in the production of bremsstrahlung by longitudinally polarized electrons. For the energies used in the present measurements, asymmetries are expected (9) to be very small ($\leq 1 \times 10^{-9}$).[5] Effects from direct electron–nucleon neutral current weak interactions are suppressed by the very low momentum transfers used in the present measurement. Effects from the weak nucleon–nucleon interaction are also expected to be very small. They would contribute through inelastic scattering to parity-mixed nuclear states and are suppressed because the inelastic scattering is such a small part of the total cross section at these energies (9).

It is interesting to consider future possibilities for improvements to a measurement of this type.

First, more stringent controls could be imposed on intensity changes upon polarization reversal. We had developed two feedback systems that controlled ion-laser intensity or Pockels cell voltage. These systems reduced $A$ values for beam intensity to less than $1 \times 10^{-5}$, but they introduce some beam motion and therefore were not used during final running. We were restricted to operation at a beam location with no energy-analyzing magnet and therefore had to resort to an independent detector to measure energy changes. The statistical and systematic accuracy in determining beam energy could therefore be improved in a future measurement.

Although we operated with average beam currents about five times higher than other pulsed polarized electron sources, our quantum efficiency for the gallium arsenide photoemitter was typically about $1 \times 10^{-3}$. Extensive development work on beam optics in the source would probably enable operation at currents of tens of milliamperes, as we had originally hoped. To date, development work on other photoemission materials for 100% electron polarization has been unsuccessful. However, several approaches are still under investigation. Therefore, it is possible to consider future measurements with techniques similar to those used in the present measurement but having improved intensity, polarization, and control of systematics. In turn, this could improve the measurement accuracy by a substantial amount. With a major effort, it might be possible to reach a sensitivity comparable with the present theoretical predictions of parity-violating effects, $\leq 5 \times 10^{-8}$ in the photodisintegration of $D_2O$.

## Acknowledgements

We would like to thank R. H. Toone and J. G. V. Taylor for their extensive work on the BIC detectors and Charles Sinclair and Dan Pierce for their guidance in the development of the polarized electron source.

1. J. M. POTTER et
YER et al. Phys.
Rev. Lett. 57, 1
2. R. WILSON et al
3. V. M. LOBASHO
4. V. A. KNYAZKO
5. E. G. ADELBERG
Sci. 35, 501 (19
6. B. DESPLANQUE
Phys. (N.Y.), 1

1. J. M. Potter *et al.* Phys. Rev. Lett. **33**, 1307 (1974); R. Balyer *et al.* Phys. Rev. C, **30**, 1409 (1984); V. Yuan *et al.* Phys. Rev. Lett. **57**, 1680 (1986).
2. R. Wilson *et al.* NBS Spec. Publ. (U.S.), 711, 85 (1986).
3. V. M. Lobashov *et al.* Nucl. Phys. **A197**, 241 (1972).
4. V. A. Knyazkov *et al.* Nucl. Phys. **A417**, 209 (1984).
5. E. G. Adelberger and W. C. Haxton. Annu. Rev. Nucl. Part. Sci. **35**, 501 (1985).
6. B. Desplanques, J. F. Donoghue, and B. R. Holstein. Ann. Phys. (N.Y.), **124**, 449 (1980).
7. H. C. Lee. Phys. Rev. Lett. **41**, 843 (1978).
8. T. Oka. Phys. Rev. D, **27**, 523 (1983).
9. B. K. Kerimov and M. Y. Safin. Sov. J. Nucl. Phys. (Engl. Transl.), **42**, 433 (1985).
10. C. Y. Prescott *et al.* Phys. Lett. **77B**, 347 (1978).
11. E. D. Earle *et al.* Nucl. Phys. **A396**, 221 (1983).
12. J. F. Lynch, R. B. Shields, and P. G. Coulter. IEEE Trans. Nucl. Sci. **NS–24**, 692 (1977).

Modern Physics Letters A, Vol. 5, No. 22 (1990) 1703–1715
© World Scientific Publishing Company

# PARITY VIOLATION IN FEW-NUCLEON SYSTEMS: WHERE DO WE STAND?*

ULF-G. MEIßNER†

*Universität Bern, Institut für Theoretische Physik, Sidlerstr. 5, CH-3012 Bern, Switzerland*

Received 29 June 1990

We review the present status of our understanding of parity violation in few-nucleon systems. At low energies, nuclear parity-violating forces can be parametrized in the framework of meson-exchange potentials. The pertinent weak meson-nucleon couplings can be calculated by invoking either the quark or the soliton model of the low-lying baryons. We compare the resulting couplings and discuss the advantages and limitations of both approaches. Then, we turn to the experimental study of nuclear parity violation in few-nucleon systems. First, we review various calculations of the longitudinal asymmetry in proton-proton scattering with an eye on the upcoming high-precision experiment at TRIUMF. We stress the importance of a consistent calculation of the weak and strong nucleon-nucleon potential. A toy calculation is presented for the photo-disintegration of the dueteron, which appears to be an excellent candidate to pin down the parity-violating pion-nucleon coupling constant. We encourage further theoretical as well as experimental studies.

## 1. Introduction

Few-nucleon systems are not only the testing ground to probe our knowledge about the strong nucleon-nucleon ($NN$) force, but are also the unique tool to study the non-leptonic, strangeness-conserving part of the weak (parity-violating) interactions. With the sophisticated parametrizations of the strong force between two nucleons existing nowadays,[1,2] we are at a point where we can test our understanding of the hadronic weak interactions in terms of meson exchange.

Much like the semi-phenomenological boson-exchange models of the strong $NN$-interaction, at low energies the parity-violating ($p\upsilon$) component of the $NN$ force can be parametrized in terms of meson exchange. Direct $W$- or $Z$-boson exchange is wiped out by the hard core of the $NN$ force, and the meson-exchange picture is a good representation of the long-range component of the $p\upsilon$-interaction. In Fig. 1, a typical Feynman diagram contributing to the $p\upsilon$ $NN$ force is shown. It is parametrized through strong and weak meson-nucleon interaction regions, $g_{MNN}(q^2)$ and $h_{MNN}(q^2)$, respectively. Because of CP invariance, uncharged scalar or pseudoscalar mesons cannot couple to on-shell nucleons, so one is left with the coupling of charged pions and the vector mesons $\rho$ and $\omega$. In the one-boson-exchange approximation, the scalar-isoscalar "$\sigma$"-meson, which accounts for the intermediate range attraction of the strong $NN$ force, does not contribute to the $p\upsilon$ interaction. The role of the $\phi$-meson is less clear. Its coupling to the nucleon is

* Work supported in part by Deutsche Forschungsgemeinschaft and by Schweizerischer Nationalfonds.
† Heisenberg fellow.

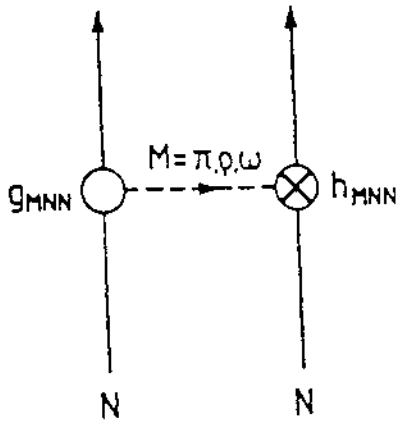


Fig. 1. Weak, parity-violating ($h_{MNN}$) and strong, parity-conserving ($g_{MNN}$) meson-nucleon vertices of the inter-nucleon potential in the one-boson-exchange framework.

nerally considered to be small (OZI-suppressed)[3] but this might be too simplistic approach in the light of the discussions surrounding the admixture of strange erators to the proton's wavefunction.[4,5]

The strong and weak meson-nucleon interaction regions can be calculated in ther the quark model[6,7] or the topological chiral soliton model of the nucleon.[8,9] In ec. 2, we will describe briefly these calculations and compare their results. Furermore, the topic of the form factors (sizes) of the meson-nucleon vertices is scussed and some remarks are made on $pv\,M\Delta N$ and $M\Delta\Delta$ vertices, which have ecently been calculated systematically within the framework of the topological hiral soliton model.[9] These vertices play an important role for energies above the ion-production threshold.

Since these $pv$ effects can only be detected in a strongly interacting system, it is andatory to look at few-nucleon systems where the strong interactions can be ontrolled. The best example of such a probe is the $pv$ analyzing power in polarized roton-proton scattering. In Sec. 3, the present status of experimental and theoretial knowledge is discussed together with some remarks on the upcoming highrecision measurement at TRIUMF. The following section deals with another few-ucleon system, namely the deuteron. A toy calculation is presented for the circular symmetry in the deuteron photo-disintegration which appears to be a very good candidate to pin down the strength of the $pv\,\pi N$ coupling, which has not been constrained considerably by present experiments apart from the $^{18}$F-experiment.[10] We also make some comments about deuteron electro-disintegration and neutron capture in hydrogen. It seems that theoretical and experimental efforts are very much needed to lead to a better understanding of the $pv\,NN$ interaction. We end this comment with a short summary and outlook.

## 2. Weak Meson-Nucleon Vertices

Here, we will summarize our present knowledge about the weak (parity-violating) meson-nucleon interaction regions. We will briefly discuss the two most recent approaches to calculate the pertinent coupling constants. For the sake of

completeness, let us defi

$$\mathcal{H}^{pv} = \frac{G_\pi}{\sqrt{2}}\,\overline{N}$$

$$+\,\overline{N}\Big[\,.$$

$$+\,h_\rho'^{1}\,\overline{N}$$

$$+\,\overline{N}\,[$$

Here, $N$ denotes a nucle
isospin matrices. The sup
refer to the change in is
any coupling between n
considered the $\phi NN$ co

The quark model calc
been pioneered by De
reconsidered by Dub
model of the strong inte
and current algebra. In
The factorization term
vertices; for the pion on
of the conserved vector

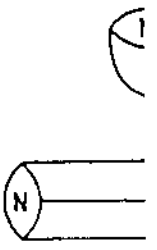


Fig. 2. Quark model diagra
categories, the so-called (a)

* In contrast to most article
pion decay constant and no

completeness, let us define the standard $pv$ meson-nucleon Hamiltonian[6,10,a]:

$$\begin{aligned}\mathcal{H}^{pv} = {} & \frac{G_\pi}{\sqrt{2}} \overline{N} [\tau \times \pi]_3 N \\ & + \overline{N} \left[ h_\rho^0 \tau \cdot \rho^\mu + h_\rho^1 \rho_3^\mu + \frac{h_\rho^2}{2\sqrt{6}} (3\tau_3 \rho_3^\mu - \tau \cdot \rho^\mu) \right] \gamma_\mu \gamma_5 N \\ & + h_\rho'^1 \overline{N} [\tau \times \rho^\mu]_3 \frac{\sigma_{\mu\nu} q^\nu}{2M} \gamma_5 N \\ & + \overline{N} [h_\omega^0 \omega^\mu + h_\omega^1 \tau_3 \omega^\mu] \gamma_\mu \gamma_5 N . \end{aligned} \tag{2.1}$$

Here, $N$ denotes a nucleon spinor, $M$ is the nucleon mass and $\tau$ the conventional isospin matrices. The superscripts '0, 1, 2' on the meson-nucleon coupling constants refer to the change in isospin ($\Delta I$) of the respective vertex. CP invariance forbids any coupling between neutral $J = 0$ mesons and on-shell nucleons, and we have not considered the $\phi NN$ coupling here.

The quark model calculation of the coupling constants $G_\pi$, $h_\rho^{0,1',1,2}$ and $h_\omega^{0,1}$ has been pioneered by Desplanques, Donoghue and Holstein (DDH)[6] and recently reconsidered by Dubovik and Zenkin (DZ).[7] Their approach is based on the quark model of the strong interaction and incorporates symmetry techniques like $SU(6)_w$ and current algebra. In Fig. 2, we show the class of diagrams considered by DDH. The factorization terms (Fig. 2a) give essential contributions to the weak $VNN$ vertices; for the pion one gets only a contribution from the neutral currents because of the conserved vector current. The so-called quark model terms shown in Fig. 2b

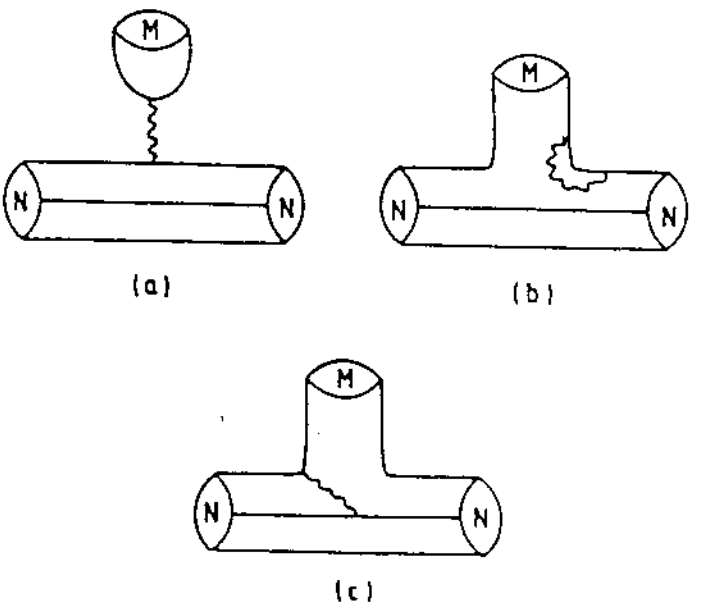


Fig. 2. Quark model diagrams to calculate the $pv$ $MNN$ vertices. These diagrams are classified in three categories, the so-called (a) factorization, (b) quark model, and (c) sum rule terms.

[a] In contrast to most articles in the current literature, we will use the symbol $f_\pi$ exclusively for the weak pion decay constant and not for the $pv$ pion-nucleon coupling, which we denote by $G_\pi$.

equire the use of specific wavefunctions, since they cannot be linked to known trangeness-changing charged current amplitudes. This, however, is the case for the o-called sum rule terms (Fig. 2c), which can be related to $\Delta S = 1$ hyperon decays y the use of $SU(6)_W$ and PCAC. For the pion, the charged current contributions tem entirely from the sum rule terms and are suppressed by $\sin^2 \theta_C \approx 1/20$. The eutral currents, however, give a pion amplitude which is proportional to $\cot \theta_C$ nd therefore enhanced.

Uncertainties in the evaluation of these diagrams come in at various places. First, ince one starts from the standard model $SU(3)_c \times SU(2)_L \times U(1)$, hard gluon xchange modifies the coefficients of the four-quark operators according to the enormalization group techniques. These corrections have, however, only been vorked out in the leading-log approximation, which generates an uncertainty of a actor of two. Further uncertainties stem from the limited knowledge about the bsolute quark masses and the model dependence of the radial integrals needed in he evaluation of the quark model terms. In Ref. 7, it is argued that some of these ncertainties can be avoided by a self-consistent approach, with particular empha- is on the MIT bag model calculation. This calculation should be redone by the hiral bag model practitioners,[11] since the pseudo-Goldstone character of the pion as always posed a problem to quark model enthusiasts.[12] Therefore, the crucial $\Delta I = 1$ $\pi NN$ coupling calculated by this approach should be considered approxima- ive. This, and other problems, actually lead DDH to consider "reasonable ranges" nd define a best value based upon their theoretical prejudices. On the positive ide, one has to remark that one starts from the truly fundamental theory of strong nd electroweak interactions and therefore directly tests its consequence. This approach is ambitious and it remains questionable whether our present day knowl- edge of the quark-gluon dynamics can go beyond the work of DDH.

Less ambitious, but better suited to incorporating chiral symmetry constraints, is the topological chiral soliton model of the nucleon. There, nucleons emerge as quantized solitons of an underlying nonlinear meson theory with interacting pions and vector mesons. Such an approach is motivated by the large $N_c$ picture advocated by Witten and 't Hooft,[13] and has been proven successful in describing many nucleon properties and linking phenomenological concepts like boson exchange or vector-meson dominance.[14] The weak meson-nucleon couplings follow straightforwardly once one has constructed the nucleon as a soliton. The starting point is the current × current form of the standard electroweak model, which can be rewritten in terms of the vector and axial-vector currents of the soliton. These currents follow uniquely by Noether's procedure and are functionals of the underlying meson fields. One can then read off the pertinent vertices by expanding these meson fields around the soliton background and picking out the terms linear in the fluctuations. These uniquely determine the couplings with no adjustable parameters. In a similar way, one can also derive the equivalent strong meson-nucleon vertices, and this is certainly one of the strong points of the soliton scenario. In the quark model, no simultaneous calculation of weak and strong vertices exists.

Of course, the soliton picture is hampered by a variety of problems. First, for meson parameters taken on their empirical values, the soliton mass generally

comes out too large by
classical quantization
classical soliton. The st
unambiguously in the
the non-perturbative c
of the fundamental q
accuracy of the solito
only been done within
$SU(3)_f$ will check out v
are fairly well reprodu

In Table 1, we co
constants. The two qu
soliton picture gives a
$N_c$ scenario, one can
suppressed. Despite tl
the quark model calc
plings, which are
calculations, altho
couplings, a trend opp
model values lie withi
the values obtained
noted, that a phenom
of $G_\pi$ if one excludes
parity-mixing in $^{18}F$ an
been derived:[10] $G_\pi \leq$
how this bound is o
structure calculation
remarks on the $pp$ ve

Ta
un
ca
wi
(D
va
st
(R

$h^1_\rho$
$h^2_\rho$
$h'_\rho$
$h^0_\omega$
$h^1_\omega$

comes out too large by several hundred MeV. This can be traced back to the semi-classical quantization in which the nucleon arises as a rotational excitation of the classical soliton. The strong interaction enhancements, which can be included fairly unambiguously in the quark model calculations, are only approximately present in the non-perturbative currents of the soliton. In Ref. 15, it was argued that changes of the fundamental quark couplings induce effects which are within the typical accuracy of the soliton scenario. Also, the soliton model calculations have so far only been done within chiral $SU(2)_f$, so it remains to be seen how the extension to $SU(3)_f$ will check out with the empirically known $\Delta S = 1$ hyperon amplitudes, which are fairly well reproduced within the quark model calculations.

In Table 1, we compare the existing calculations of the $pv$ meson-nucleon constants. The two quark model calculations give comparable results, whereas the soliton picture gives a considerably reduced weak $\pi NN$ coupling. Within the large $N_c$ scenario, one can show the $G_\pi/h_\rho^0 \sim O(1/N_c)$,[15] i.e., the weak $\pi NN$ coupling is suppressed. Despite the fact that $N_c = 3$, the soliton model obeys this rule, whereas the quark model calculations give $G_\pi$ comparable to $h_\rho^0$. The vector meson couplings, which are subject to less uncertainties than $G_\pi$, are comparable in all calculations, although in the soliton model the $\omega$ couplings are larger than the $\rho$ couplings, a trend opposite to the quark model. It is amusing to note that all soliton model values lie within the "reasonable ranges" defined by DDH, whereas some of the values obtained by DZ are outside these ranges. It should be furthermore noted, that a phenomenological fit to the most reliable $pv$ data favors a small value of $G_\pi$ if one excludes the $^{21}$Ne-data,[10] which are quite uncertain. Also, from the parity-mixing in $^{18}$F and the first forbidden $\beta$-decay in $^{19}$F, an upper bound for $G_\pi$ has been derived:[10] $G_\pi \leq 1.43 \times 10^{-7}$, well below the DDH value. For more details on how this bound is obtained and the degree of self-consistency of the nuclear structure calculations involved, the reader should consult Ref. 10. Two more remarks on the $pv$ vector couplings are in order. First, the relatively large value of

Table 1. Weak meson-nucleon coupling constants in units of $10^{-7}$. We present the result of the soliton model calculation of Kaiser and Meißner (KM)[8,9] together with the quark model results of Desplanques *et al.* (DDH)[6] as well as Dubovik and Zenkin (DZ).[7] The value for $h_\rho^{\prime 1}$ in the column DDH is taken from Holstein's calculation in Ref. 19. The "reasonable ranges" (*RR*) defined by DDH are also given.

| | KM | DDH | DZ | RR |
|---|---|---|---|---|
| $G_\pi$ | 0.2 | 4.5 | 1.3 | $0.0 \to 11.4$ |
| $h_\rho^0$ | $-3.7$ | $-11.4$ | $-8.3$ | $-30.8 \to 11.4$ |
| $h_\rho^1$ | $-0.1$ | $-0.2$ | $+0.4$ | $-0.4 \to 0.1$ |
| $h_\rho^2$ | $-3.3$ | $-9.5$ | $-6.7$ | $-11.0 \to -7.6$ |
| $h_\rho^{\prime 1}$ | $-2.2$ | $-0.7$ | 0.0 | |
| $h_\omega^0$ | $-6.2$ | $-1.9$ | $-3.9$ | $-10.3 \to +5.7$ |

obtained in the soliton model is close to the best-fit estimate of Adelberger and axton in Ref. 10. Second, for the $\rho$ couplings, the quark and soliton model gives $> h_\rho^2 \gg h_\rho^1$, in agreement with the large-$N_c$ counting rules $h_\rho^0 : h_\rho^2 : h_\rho^1 = 1 : \sin^2(\theta_W)$ $\sin^2(\theta_W)/N_c$ derived in Ref. 15. It should also be noted that isovector two-pion xchange gives only small corrections to the one-rho contributions.[46]

Up to now, we have considered only amplitudes like $\langle NM | \mathcal{H}^{pv} | N \rangle$ with $M = \pi$, $\omega$. We know, however, from the boson-exchange picture of the strong $NN$ force, at correlated two-pion exchange with intermediate $\Delta(1232)$-resonances is of tmost importance to generating the intermediate range attraction between two ucleons. In the quark model, no systematic investigation of the $M\Delta N$ vertices has een performed so far.[b] In the soliton model, where the $\Delta(1232)$ is a rotational xcitation of the classical soliton much like the nucleon, it is an easy exercise to valuate these couplings.[9] The findings presented in Ref. 9 can be summarized as llows: Generally, $M\Delta N$ and $M\Delta\Delta$-couplings are comparable to their $MNN$ ounterparts. In the case of the $\pi\Delta N$ coupling, the isoscalar coupling vanishes, hereas the isovector coupling is comparable to $G_\pi$. At small $q^2$, it is of course ppressed by the kinematical factor of $q^2/4M^2$, but such an argument cannot be sed anymore when one considers, e.g., two-pion exchange with intermediate $\Delta$'s. seems therefore very necessary to redo the calculation of Ref. 17 to find out the eight of the parity-violating $M\Delta N$ and $M\Delta\Delta$ vertices.

Another topic to be addressed is the finite extent of the weak meson-nucleon nteraction regions. These are of utmost importance to regularizing the singular ehavior of the $pv$ potential at short distances, quite analogous to the form factors n the strong meson-exchange potentials.[1,2,c] In the soliton model, strong and weak orm factors can be calculated simultaneously and it turns out that these form actors are of the monopole type with cutoffs $\Lambda \approx 5$ fm$^{-1}$. Also the weak $MNN$ form actors are similar to the equivalent strong ones. For the $\pi NN$ vertex, which ominates the long-range part of the weak and strong $NN$ interactions, the soliton nodel predicts a weak form factor with a cutoff $\Lambda_\pi^W = 0.98$ GeV and a strong one vith a cutoff $\Lambda_\pi^S = 0.86$ GeV. The latter number is not far from the results on the trong $\pi NN$ vertex obtained from charge-exchange reactions in light nuclei.[18] The roximity of these cutoffs can be understood from the fact that the $\pi NN$ vertex weak or strong) is essentially regulated by the extension of the pion-field building p the soliton, $\Lambda \approx \sqrt{6}/r_B \approx 1$ GeV, since $r_B \approx 0.5$ fm. It would be very useful to erform a similar calculation in the quark model to see whether the soliton predicion can be considered a genuine result.

## 3. Parity Violation in Proton-Proton Scattering

The simplest system in which one can probe certain components of the weak $pv$ nter-nucleon force is the two-nucleon system as first pointed out by Simonius[20] and Lee. By scattering polarized protons off a hydrogen target, parity violation mani-

fests itself in a non-va

when the beam is 100
of. $\sigma^\pm$ are the cross-se
the unpolarized targe
also sensitive to the st
argument. To calculat
first pioneered by Bro
strong and a weak par
nucleon system. Now
distortions, i.e., one h
waves, $\mathcal{F}_{ss'}^W \propto \langle \psi_s^{(-)} | V$
energy dependence o
distortions. Therefore
weak potential. Such
based on the Bonn
that the weak pion-
exchange approximat
tially tests the weak v

In Ref. 23, not only
used, but also the sol
Zenkin. The resulting
predicted by the solit
by the low energy dat
3 gives $\chi^2 = 34/3$ (DI
energy at which the a
predicts, which can be
contrast to the quark
at $E_{lab} = 222$ MeV.
$pp$ parity violation m
energy and therefore
measurement of the c
tion of the weak vec
various weak parame
potential, the predict

[b] Some educated guesses can be found in Ref. 16 and traced back from there.

[c] In the Paris potential no form factors are used but a phenomenological parametrization for small separation does the job.

[d] A recent measurement
$A_L = (-1.49 \pm 0.54) \times 10^{-}$
[e] In Ref. 25, a calculation u
find $A_L$ (230 MeV) = + 7 ×

fests itself in a non-vanishing asymmetry,

$$A_L = \frac{\sigma^+ - \sigma^-}{\sigma^+ + \sigma^-}, \tag{3.1}$$

when the beam is 100% polarized and Coulomb corrections have been taken care of. $\sigma^\pm$ are the cross-sections for scattering positive/negative helicity protons from the unpolarized target. This observable does not only test the $p\upsilon$ potential, but it is also sensitive to the strong inter-nucleon forces, as can be seen from the following argument. To calculate this process in the distorted-wave Born-approximation, as first pioneered by Brown *et al.*,[21] one splits the total scattering amplitude $\mathcal{F}_{ss'}$ into a strong and a weak part: $\mathcal{F}_{ss'} = \mathcal{F}^{S}_{ss'} + \mathcal{F}^{W}_{ss'}$. Here, $s$ and $s'$ are the total spins of the two-nucleon system. Now it is of utmost importance to take into account the strong distortions, i.e., one has to calculate the weak scattering amplitude with distorted waves, $\mathcal{F}^{W}_{ss'} \propto \langle \psi_s^{(-)} | V_{p\upsilon} | \psi_{s'}^{(+)} \rangle$, with $V_{p\upsilon}$ the $p\upsilon$ one-meson-exchange potential. The energy dependence of the analyzing power $A_L$ is entirely determined by the strong distortions. Therefore, it is mandatory to consistently calculate the strong and the weak potential. Such a procedure was recently worked out by Driscoll and Miller[22] based on the Bonn potential for the strong interactions. We should point out here that the weak pion-nucleon vertex does not contribute to $A_L$ in the one-boson-exchange approximation because of isospin conservation. One therefore essentially tests the weak vector meson couplings $h_\rho^{pp} = h_\rho^0 + h_\rho^1 + h_\rho^2/\sqrt{6}$ and $h_\omega^{pp} = h_\omega^0 + h_\omega^1$.

In Ref. 23, not only the quark model values of DDH for the weak couplings were used, but also the soliton model results as well as the predictions of Dubovik and Zenkin. The resulting curve for $A_L$ is shown in Fig. 3. The shape of the curve as predicted by the soliton model follows more closely the empirical trend suggested by the low energy data.[24,d] In fact, a $\chi^2$ calculation for the three curves shown in Fig. 3 gives $\chi^2 = 34/3$ (DDH, best values), $\chi^2 = 26/3$ (DZ) and $\chi^2 = 8/3$ (KM).[44] The energy at which the asymmetry changes sign is larger than what the quark model predicts, which can be traced back to the fact that in the soliton model $h_\omega^{pp} > h_\rho^{pp}$, in contrast to the quark model giving $h_\omega^{pp} < h_\rho^{pp}$. Of particular interest is the value of $A_L$ at $E_{lab} = 222$ MeV. This is the energy selected for an upcoming high-precision $pp$ parity violation measurement at TRIUMF because $\delta(^3S_0) + \delta(^3P_0) = 0$ at this energy and therefore the $J = 0$ contribution to the analyzing power vanishes. The measurement of the dominant $J = 2$ contribution gives access to another combination of the weak vector meson couplings already measured at 45 MeV. For the various weak parameters summarized in Table 1 together with the strong Bonn potential, the predictions for $A_L$ at 222 MeV are[e]

$$\begin{aligned} A_L(\mathrm{DDH}) &= 5.0 \times 10^{-8}, \\ A_L(\mathrm{DZ}) &= 2.6 \times 10^{-8}, \\ A_L(\mathrm{KM}) &= 3.7 \times 10^{-9}. \end{aligned} \tag{3.2}$$

[d] A recent measurement of $A_L$ at 14.5 MeV is carried out at Bonn.[35] The preliminary result of $A_L = (-1.49 \pm 0.54) \times 10^{-7}$ is consistent with the 15 MeV data.[24]

[e] In Ref. 25, a calculation using the DDH parameters and the Paris potential is presented. These authors find $A_L$ (230 MeV) $= +7 \times 10^{-9}$, but the weak and strong potentials are not consistently derived.

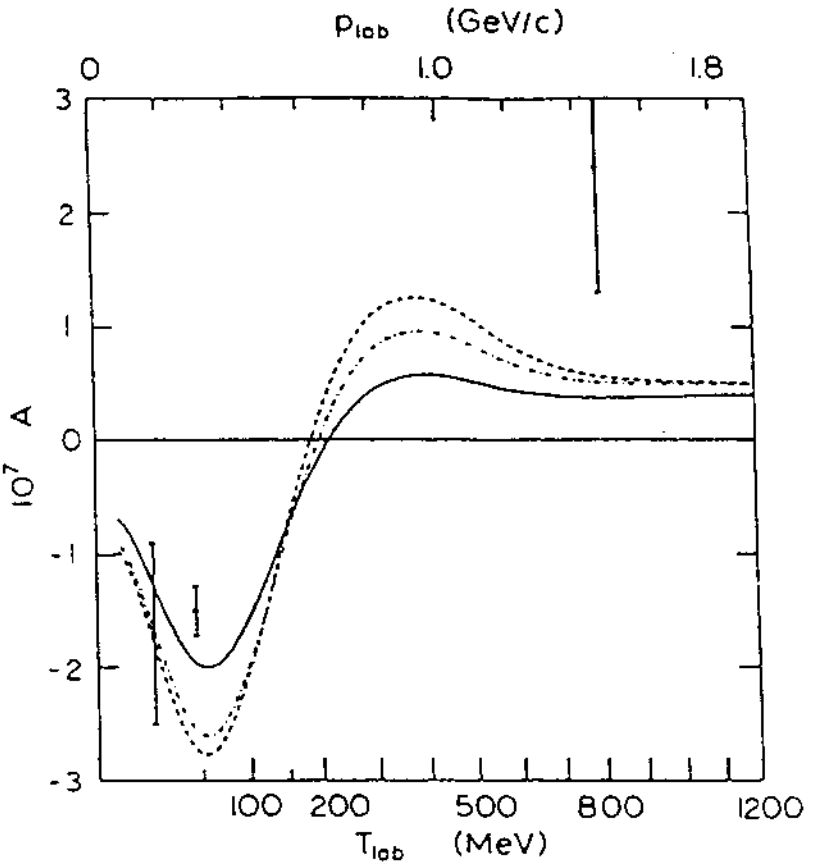


ig. 3. Parity-violating asymmetry in $pp$ scattering. The solid line gives the prediction based on the weak ouplings as given by the soliton model,[8] whereas the dashed and dash-dotted lines are based on the uark model calculations of Refs. 6 and 7.

So the quark[6] and soliton model predictions differ by $\Delta A_L \simeq 4.6 \times 10^{-8}$. It should be noted that the projected long-term accuracy of the TRIUMF experiment is $(\delta A_L)_{stat} \simeq \pm 1 \times 10^{-8}$,[26] which should be sufficient to discriminate between these predictions. This experiment should set rather stringent limits on certain combinations of the weak $\rho NN$ and $\omega NN$ couplings.

Let us now discuss the analyzing power for $p_{lab} \geq 1$ GeV/$c$. All curves underestimate considerably the measured data at $T_{lab} = 0.8$ GeV.[27] This is not surprising since inelastic effects, taken into account only by use of strong phase shifts and two-pion exchange with intermediate $N$ and $\Delta$ states, will become important at these energies. These processes are recently under investigation by Driscoll and Miller.[28] A first attempt to study the effect of charged pion exchange which results in a $n\Delta^{++}$ state has been undertaken by Silbar *et al.*[29] They find a sizable effect even below pion production threshold when they use the weak pion-nucleon coupling constant of DDH.[f] However, parity-violating $\pi\Delta N$ and $\pi\Delta\Delta$ vertices are neglected and

[f] The effect calculated in Ref. 29 scales linearly with $G_\pi$. If one had used the weak $\pi NN$ coupling as predicted by the soliton model, this effect would be fairly small for all relevant energies. Recently, the calculation of Ref. 29 has been redone by Kloet, Silber and Tjon[45] with a better strong interaction model, which leads to an improved description of the lower partial waves. For the $pp$ asymmetry, the overall $2\pi$ effect is reduced by a factor 5 at 500 MeV and by a factor 2 at 800 MeV.

heavy meson exchang
considered indicative
$\pi NN$ coupling is as la
complicate the analy
thorough study of $2\pi$-
was even argued that
calculation, however,
form factors taken f
Furthermore, the ove
understanding of this
Refs. 22 and 28, we s
the intermediate-ran
scattering.

Finally, we shoul
protons with momen
$\times 10^{-7}$.[39] This value c
present. First, let us
Henley[40] has sho
order of magnitude s
and mixing between
ing model is present
overall normalizatio
that $A_L$ grows consid
Simonius and Unger
due to an inconsiste
diquark scattering. F
used in Ref. 41, $A_L$
empirical value. It, t
of the Argonne exp

## 4. Deuteron Disint

As it was stresse
physics in a few-nuc
violating weak effec
which can be calcula
present a simple est

with left/right circu
this process using
dipole transitions w
We will later comm
rized as follows.

heavy meson exchange is not considered. Therefore, these results should only be considered indicative and a full scale calculation has to be performed. If the weak $\pi NN$ coupling is as large as that predicted by DDH, charged pion-exchange would complicate the analysis of the upcoming TRIUMF experiment. Also, a more thorough study of $2\pi$-exchange at low energies is very much needed. In Ref. 37, it was even argued that $2\pi$ exchange plays an important role at 15 and 45 MeV. This calculation, however, does not consistently derive weak and strong potentials, and form factors taken from the chiral/cloudy bag model have been added *ad hoc*. Furthermore, the overall effect scales with $G_\pi$ and is therefore subject to our limited understanding of this coupling. With the on-going investigation of the authors of Refs. 22 and 28, we should soon have a better (more consistent) understanding of the intermediate-range $pv$ potential and its contribution to the asymmetry in $pp$ scattering.

Finally, we should point onto the Argonne experiment in which polarized protons with momentum of 6 GeV/$c$ are scattered off $H_2O$ giving $A_L = (26.5 \pm 6.0) \times 10^{-7}$.[39] This value of the asymmetry cannot be explained by any mechanism at present. First, let us faithfully trust meson exchange up to such high energies. Henley[40] has shown that relativized meson exchange leads to a result which is an order of magnitude smaller than the empirical value even if one neglects absorption and mixing between various channel. However, in Ref. 41 a quark-diquark scattering model is presented which appears to explain this large value of $A_L$. Since the overall normalization is hard to fix in this approach, the most prominent feature is that $A_L$ grows considerably as the energy increases up to some hundreds of GeV. Simonius and Unger[42] have shown that the increase of $A_L$ with energy in Ref. 41 was due to an inconsistent treatment of all Feynman diagrams contributing to quark-diquark scattering. Furthermore, they showed that, with the same parameters as used in Ref. 41, $A_L \leq 2 \times 10^{-7}$, i.e., being again one order of magnitude below the empirical value. It, therefore, remains a theoretical challenge to explain the result of the Argonne experiment.[39]

## 4. Deuteron Disintegration and the $n$-$p$ System

As it was stressed before, only a good knowledge of the strong interaction physics in a few-nucleon system can lead one to a good understanding of parity-violating weak effects. So let us turn our attention to another two-nucleon system which can be calculated quite reliably, namely the deuteron. In particular, we will present a simple estimate of the circular asymmetry in the reaction

$$\gamma + d \rightarrow n + p \tag{4.1}$$

with left/right circularly polarized photons. Oka[30] has performed a calculation of this process using the Hamada-Johnston potential[31] and restricting himself to dipole transitions when calculating the cross-section for the photo-disintegration. We will later comment on these assumptions. The result of Ref. 30 can be summarized as follows,

$$A_L(\omega) = -2\alpha F_0 - 2\alpha' G_0 - 2\beta F_2 - 2\gamma(F_1 - G_1) - 4\gamma' H_1 + \sqrt{32}\,\delta F_\pi\,, \quad (4.2)$$

ı $\alpha$, $\beta$,..., $\delta$ being energy-dependent coefficients and $F_\pi$, $F_0$, $G_0$,... the conven-ıal products of weak and strong coupling constants, $F_\pi = g_{\pi NN}\, G_\pi/\sqrt{32}$, $F_{0,1,2} = 2\, g_{\rho NN}\, h_\rho^{0,1,2}$, $G_{0,1} = -1/2\, g_{\omega NN}\, h_\omega^{0,1}$ and $H_1 = -1/4\, g_{\rho NN}\, h'^1_\rho$. Here, $g_{MNN}$ ($M = \pi, \rho,$ are the usual strong meson-nucleon coupling constants ($g_{\pi NN} = 13.45$, $g_{\rho NN} = 3.25$, $_\omega = 15.9$, e.g., in the Bonn potential). $\omega = \omega_L - E_B$, with $E_B = 2.22$ MeV being the ıteron binding energy, is the incident photon energy.

n Fig. 4, we show $A_L(\omega)$ for 1 MeV $\leq \omega \leq$ 30 MeV for the various weak couplings ined in Sec. 2 and the strong couplings used by Oka.[30] The dashed line gives the diction of the soliton model when the strong parameters as predicted by it are d. The quark model parameters of DDH and DZ essentially give rise to a linear ɔendence of $A_L(\omega)$ as $\omega$ increases, with the slope determined by the strength of $p\upsilon\ \pi NN$ coupling. For the DDH case the pion contribution is completely ninant for all energies, whereas for the DZ parameters the reduced $\pi NN$ ɜngth leads to an overall decrease of $A_L(\omega)$. For the soliton model, however, ngs are significantly different. First, between 1 and 20 MeV, $A_L(\omega)$ shows a flat nimum at about $\omega_L \approx 12$ MeV, and only after $\omega_L \geq 20$ MeV a gradual rise in $A_L(\omega)$ s in. Also, the overall magnitude of the effect is an order of magnitude smaller

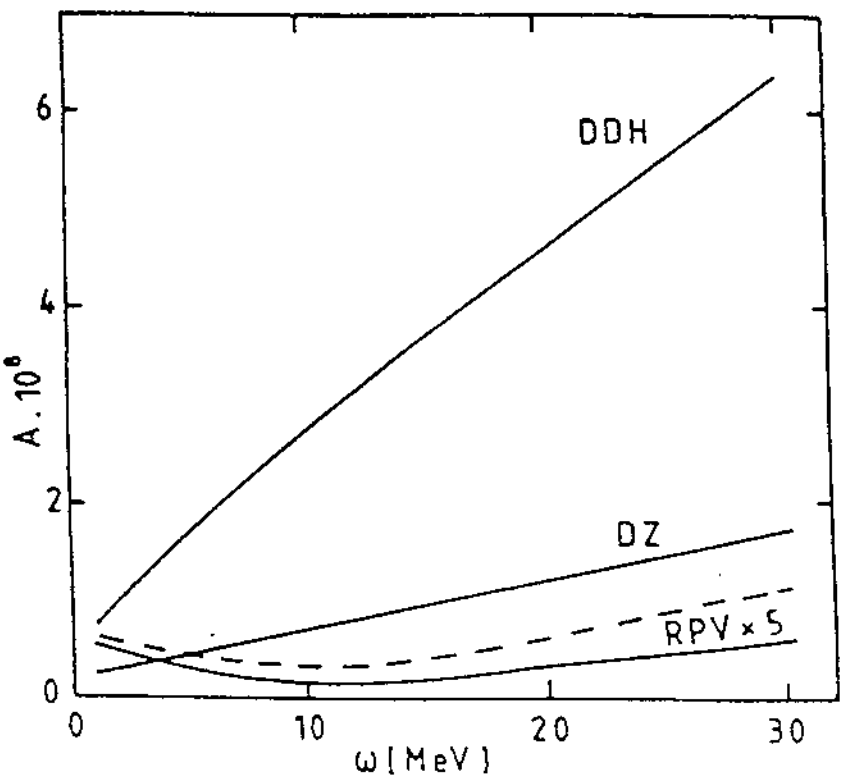


ig. 4. Parity-violation in the deuteron photo-disintegration. We show the circular asymmetry for ıotons with incident energy $\omega$ for various sets of weak meson-nucleon couplings: DDH,[6] DZ[7] and PV,[8] based on the calculation of Ref. 30. For the dashed line, the strong coupling constants as pre-icted by the chiral soliton model have been used. Notice that both soliton curves ("RPV") are ıagnified by a factor five.

for the weak paramete
measure the asymmetr
is small the tremendc
dedicated experiment.
cal study has also to be
the Bonn potential anc
formed. Second, the ef
role in an accurate de
Therefore, the results
the trends exhibited wi

As the incident phc
balances, the circular
photon circular polariz
$d + \gamma$. This quantity is
parameters due to the
various calculations fo
do not agree.[30,33] This
tion of the deuterc

The situation is sim
which probes other kir
do not agree[34,35] and
exchange potentials h
photon point, the as
disintegration is relat
strong constraint on
value of $P_\gamma = (1.8 \pm 1.8$
predictions. Similarly
the asymmetry of 2.2
captured by protons.
whereas for the solit
essentially reflects the
cal value of $(0.6 \pm 2.1$
high neutron fluxes fr
to get a better handl
electro-disintegration
calculated with the p
presented in Fig. 4 su
thermal neutron capt
fluxes.

## 5. Summary and Ou

Parity violation in
understanding of the

[6] For a more detailed disc

for the weak parameters predicted by the soliton model. It would be worthwhile to measure the asymmetry, say at 10 and 20 MeV incident energy, although the effect is small the tremendously different slope of $A_L(\omega)$ should be detectable in a dedicated experiment. Of course, as already mentioned, a more thorough theoretical study has also to be done. First, a more consistent calculation employing, e.g., the Bonn potential and the equivalently constructed weak potential should be performed. Second, the effects of meson-exchange currents, which play an important role in an accurate description of the deuteron properties[32] have to be included. Therefore, the results presented in Fig. 4 should only be considered as a guide, but the trends exhibited will certainly not be wiped out by a more elaborate calculation.

As the incident photon energy goes to zero and by the principle of detailed balances, the circular asymmetry measured in $\gamma + d \rightarrow n + p$ becomes equal to the photon circular polarization in the capture of thermal neutrons by protons, $n + p \rightarrow d + \gamma$. This quantity is very sensitive to the actual values of the weak and strong parameters due to the cancellation of $\omega$ and $\rho$ meson contributions. Indeed, the various calculations for the nuclear structure coefficients available in the literature do not agree.[30,33] This fact strengthens our argument that a more complete calculation of the deuteron disintegration should be performed.

The situation is similar in the case of electro-disintegration of the deuteron, which probes other kinematics than the photo-disintegration. Existing calculations do not agree[34,35] and the full machinery of the recently proposed strong boson-exchange potentials has not been used in a consistent fashion. Again, at the soft-photon point, the asymmetry in the differential cross-section of the electro-disintegration is related to the circular polarization in $n + p \rightarrow d + \gamma$. This poses a strong constraint on any calculation. From the experimental side, the measured value of $P_\gamma = (1.8 \pm 1.8) \times 10^{-9}$ [36]is still not accurate enough to limit the theoretical predictions. Similarly sensitive to the value of the weak pion-nucleon coupling is the asymmetry of 2.2 MeV photons emitted when polarized thermal neutrons are captured by protons. For the DDH parameters, the prediction is $A_\gamma = -0.49 \times 10^{-7}$, whereas for the soliton model parameters one finds $A_\gamma = -0.03 \times 10^{-7}$, which essentially reflects the small value of $G_\pi$ found in that approach. Again, the empirical value of $(0.6 \pm 2.1) \times 10^{-7}$ [43]is too inaccurate to draw any conclusion. With the high neutron fluxes from reactors like that, e.g., at Grenoble, it should be possible to get a better handle on this quantity.[8] To summarize, the deuteron photo- and electro-disintegration and the related neutron capture should be rigorously recalculated with the present day available machinery and estimates like the one presented in Fig. 4 suggest the need of dedicated experiments on the deuteron or of thermal neutron capture, which might be possible with present day reactor neutron fluxes.

## 5. Summary and Outlook

Parity violation in few nucleon systems allows for a simultaneous study of our understanding of the strong (parity-conserving) and weak (parity-violating) meson-

[8] For a more detailed discussion of other observables in the $n - p$ system see Ref. 10.

cleon interaction regions. At present, various calculations of these $pv$ meson-cleon couplings exist which differ drastically for the value of the fundamental ak pion-nucleon coupling. Present day experiments only give an upper limit on s quantity. The most commonly used value for the weak $\pi NN$ coupling based on quark model calculation of Desplanques *et al.*[6] is in conflict with this bound. The vector-meson couplings show less uncertainties, also the relative strength of $\omega$ $\rho$ couplings varies between the quark and soliton model calculations. The eoretical questions surrounding the importance of the intermediate-range contri-tions from $2\pi$-exchange should soon find a resolution in a consistent calculation the weak and strong potentials. Of course, these effects scale linearly with $G_\pi$, d this again points towards the importance of getting a better handle on the $pv$ on-nucleon interaction region.

Here, we have discussed how dedicated parity violation experiments in few-icleon systems can lead to more stringent limits on the $pv$ meson-nucleon verti-s. In particular, the proton-proton system gives information about the vector eson couplings and the correlated two-pion exchange, and it is shown that the coming TRIUMF experiment at $T_{lab}$ = 222 MeV should be very useful for scriminating between the various theoretical predictions. Furthermore, the photo-sintegration of the deuteron or thermal neutron capture at modest energies ove threshold appears to be a clear filter to pin down the value of the weak $\pi NN$ upling. It is obvious that more theoretical effort is needed to strengthen these onclusions based on a rather simple calculation. Altogether, we can be hopeful at in the next years our understanding of nuclear parity violation will go beyond e stage of "reasonable ranges" as defined by the authors of Ref. 6 ten years ago.

## cknowledgments

I would like to thank Doug Driscoll and Norbert Kaiser for fruitful collabora-ons on which this work is based and Véronique Bernard for critical reading of the anuscript. I am grateful to Wick Haxton and Ernest Henley for constructive emarks.

## References

1. M. Lacombe *et al.*, *Phys. Rev.* **C21** (1980) 861.
2. R. Machleidt, K. Holinde, and C. Elster, *Phys. Rep.* **149** (1987) 1.
3. H. Genz and G. Höhler, *Phys. Lett.* **61B** (1976) 389.
4. R. L. Jaffe, *Phys. Lett.* **229B** (1989) 275.
5. V. Bernard, in *Proc. XI Autumn School in Physics*, Lisbon, Oct. 1989, to be published.
6. B. Desplanques, J. F. Donoghue, and B. R. Holstein, *Ann. Phys. (N. Y.)* **124** (1980) 449.
7. V. N. Dubovik and S. V. Zenkin, *Ann. Phys. (N. Y.)* **172** (1986) 100.
8. N. Kaiser and Ulf-G. Meißner, *Nucl. Phys.* **A489** (1988) 671; **A499** (1989) 699.
9. N. Kaiser and Ulf-G. Meißner, *Nucl. Phys.* **A510** (1990) 759.
10. E. G. Adelberger and W. C. Haxton, *Ann. Rev. Nucl. Part. Phys. Sci.* **35** (1985) 501.
11. See, e.g., G. E. Brown and M. Rho, *Commun. Nucl. Part. Phys.* **15** (1986) 245.
12. V. Bernard *et al.*, *Nucl. Phys.* **A412** (1984) 349; *Nucl. Phys.* **A440** (1985) 605.
13. G. 't Hooft, *Nucl. Phys.* **B72** (1974) 461; *Nucl. Phys.* **B75** (1974) 461; E. Witten, *Nucl. Phys.* **B160** (1979) 57.
14. Ulf-G. Meißner, *Phy*
15. I. Grach and M. Shn
16. R. M. Gorman and I
17. See, e.g., G. N. Epst
18. C. A. Dominguez ar
19. B. R. Holstein, *Phys*
20. M. Simonius, *Phys.*
21. V. R. Brown, E. M.
22. D. E. Driscoll and C
23. D. E. Driscoll and U
24. D. E. Nagle *et al.*, *A* (1987) 1616.
25. Y. Avishai and P. G
26. S. Page, in TRIUMI
27. R. W. Harper *et al.*, 1680.
28. D. E. Driscoll and C
29. R. R. Silbar *et al.*, *F*
30. T. Oka, *Phys. Rev.*
31. T. Hamada and I. I
32. D. O. Riska and G. *Phys.* **A264** (1976)
33. B. Desplanques
34. M. Porrmann, *Nucl*
35. W. Y. P. Hwang, E
36. V. A. Knyazkov *et*
37. M. M. Musakhano
38. D. Eversheim, priv
39. N. Lockyer *et al.*, *F*
40. E. M. Henley, *Nucl* 977.
41. T. Goldman and D
42. M. Simonius and L. report 89-5, p. 20, 1
43. J. F. Caviagnac *et*
44. D. E. Driscoll, PhI
45. W. M. Kloet, R. R
46. N. Kaiser and Ulf-

14. Ulf-G. Meißner, *Phys. Rep.* **161** (1988) 213.
15. I. Grach and M. Shmatikov, *Z. Phys.* **C44** (1989) 393.
16. R. M. Gorman and B. H. J. McKellar, *Mod. Phys. Lett.* **A1** (1986) 631.
17. See, e.g., G. N. Epstein, *Phys. Lett.* **71B** (1977) 267.
18. C. A. Dominguez and B. J. VerWest, *Phys. Lett.* **89B** (1980) 333.
19. B. R. Holstein, *Phys. Rev.* **D23** (1981) 1613.
20. M. Simonius, *Phys. Lett.* **41B** (1972) 415; *Nucl. Phys.* **A220** (1974) 269.
21. V. R. Brown, E. M. Henley, and F. R. Krejs, *Phys. Rev.* **C9** (1974) 935.
22. D. E. Driscoll and G. A. Miller, *Phys. Rev.* **C39** (1989) 1951; **C40** (1989) 2159.
23. D. E. Driscoll and Ulf-G. Meißner, *Phys. Rev.* **C41** (1990), in press.
24. D. E. Nagle *et al.*, *AIP Conf. Proc.* No. 51, p. 224; S. Kistryn *et al.*, *Phys. Rev. Lett.* **58** (1987) 1616.
25. Y. Avishai and P. Grangé, *Nucl. Phys.* **A491** (1989) 677.
26. S. Page, in TRIUMF brown report 89-5, 1989.
27. R. W. Harper *et al.*, *Phys. Rev.* **D31** (1985) 1151; V. Yuan *et al.*, *Phys. Rev. Lett.* **57** (1986) 1680.
28. D. E. Driscoll and G. A. Miller, work in progress.
29. R. R. Silbar *et al.*, *Phys. Rev.* **C40** (1989) 2218.
30. T. Oka, *Phys. Rev.* **D27** (1983) 523.
31. T. Hamada and I. D. Johnston, *Nucl. Phys.* **34** (1962) 382.
32. D. O. Riska and G. E. Brown, *Phys. Lett.* **38B** (1972) 193; M. Gari and H. Hyuga, *Nucl. Phys.* **A264** (1976) 409.
33. B. Desplanques, *Nucl. Phys.* **A335** (1980) 147.
34. M. Porrmann, *Nucl. Phys.* **A360** (1981) 251.
35. W. Y. P. Hwang, E. M. Henley, and G. A. Miller, *Ann. Phys. (N. Y.)* **137** (1981) 378.
36. V. A. Knyazkov *et al.*, *Nucl. Phys.* **A417** (1984) 209.
37. M. M. Musakhanov and Y. Y. Podgornov, *Sov. J. Nucl. Phys.* **44** (1986) 459.
38. D. Eversheim, private communication.
39. N. Lockyer *et al.*, *Phys. Rev. Lett.* **45** (1980) 1821; *Phys. Rev.* **D30** (1984) 860.
40. E. M. Henley, *Nucl. Phys.* **A483** (1988) 596; see also T. Oka, *Prog. Theor. Phys.* **66** (1981) 977.
41. T. Goldman and D. Preston, *Nucl. Phys.* **B217** (1983) 61, *Phys. Lett.* **168B** (1986) 415.
42. M. Simonius and L. Unger, *Phys. Lett.* **198E** (1987) 547; M. Simonius in TRIUMF brown report 89-5, p. 20, 1989.
43. J. F. Caviagnac *et al.*, *Phys. Lett.* **67B** (1977) 148.
44. D. E. Driscoll, PhD thesis, University of Washington, 1990, unpublished.
45. W. M. Kloet, R. R. Silber, and J. A. Tjon, Los Alamos preprint, 1990.
46. N. Kaiser and Ulf-G. Meißner, Bern University preprint BUTP-90/7, 1990.

# Measurement of the Parity-Violating Gamma Asymmetry $A_\gamma$ in the Capture of Polarized Cold Neutrons by Para-Hydrogen, $\vec{n} + p \rightarrow d + \gamma$


J.D. Bowman (Spokesman), G.L. Greene, G.E. Hogan, J.N. Knudson, S.K. Lamoreaux, G.L. Morgan, C.L. Morris, S.I. Penttilä, D.A. Smith, T.B. Smith, W.S. Wilburn, and V.W. Yuan
*Los Alamos National Laboratory*

A. Bazhenov, E. Kolomenski, A. Pirozhkov, and A. Serebrov
*Petersburg Nuclear Physics Institute*

C.S. Blessinger, G. Hansen, H. Nann, D.R. Rich, and W.M. Snow
*Indiana University*

T.E. Chupp, K.P. Coulter, R.C. Welsh, and J. Zerger
*University of Michigan*

S.J. Freedman and B.K. Fujikawa
*University of California, Berkeley*

T.R. Gentile, G.L. Jones, and F.E. Wietfeldt
*National Institute of Standards and Technology*

M.B. Leuschner and V.R. Pomeroy
*University of New Hampshire*

A. Masaike and Y. Matsuda
*Kyoto University*

S. Ishimoto, Y. Masuda, and K. Morimoto
*KEK National Laboratory, Japan*

E.I. Sharapov
*Joint Institute for Nuclear Research, Dubna*



Submitted to the U.S. Department of Energy
17 April 1998

## Abstract

We propose to measure the parity-violating asymmetry $A_\gamma$ of the correlation between the direction of emission of the gamma ray $\vec{k}_\gamma$ and the neutron polarization $\vec{s}_n$ in the reaction $\vec{n} + p \rightarrow d + \gamma$. This asymmetry is expected to be $\approx 5 \times 10^{-8}$. We argue that it is possible to obtain a statistical uncertainty of $0.5 \times 10^{-8}$ at LANSCE. We argue that systematic errors are expected to be small compared to the statistical error. The symmetries of the strong, weak, and electromagnetic interactions imply that $A_\gamma$ is determined by the $\Delta I = 1$ part of the weak interaction. The sensitivity of the deuteron wave function to the long-range components of the $NN$ interaction implies that $A_\gamma$ is dominated by the longest-range $\Delta I = 1$ contribution, which is due to weak pion exchange. The asymmetry, $A_\gamma$, can therefore be related to the weak isovector pion-nucleon-nucleon coupling, $H^1_\pi$, with negligible uncertainty due to nuclear structure. (We use the definition of the weak nucleon-nucleon couplings of Adelberger and Haxton [1].) We will determine $H^1_\pi$ with an uncertainty of $1.0 \times 10^{-7}$, 10% of its expected value, $1.1 \times 10^{-6}$. At present there are two experiments; gamma ray circular polarization for $^{18}$F ($H^1_\pi < 0.3 \times 10^{-6}$) and the anapole moment of $^{133}$Cs ($H^1_\pi = 2.4 \pm 0.6 \times 10^{-6}$) that have been interpreted to give very different values of $H^1_\pi$.

There are three physics goals that this measurement addresses, matched to three different energy regimes. A measurement of $H^1_\pi$ to the proposed accuracy will fix its value, thereby resolving the current controversy. We outline a feasible and partially complete program of measurements that will over-constrain the weak $NN$ couplings. Completion of this program will finally allow parity violation measurements to be used to address questions in nuclear physics. A reliable measurement of $H^1_\pi$ is an essential part of an experimental program to over-determine the weak $NN$ couplings and thereby test the internal consistency of the meson-exchange picture of the weak $NN$ interaction. Such a test of the meson exchange picture has the potential to tell us something new about low energy QCD, especially if the meson picture fails. Finally, since the $\Delta I = 1$ flavor-conserving weak $NN$ interaction is dominated by quark-quark neutral currents at the electroweak scale, we can learn how the effective strength of quark-quark neutral currents is modified by QCD.

$$^1S_0 \longrightarrow {}^3S_1 + M_1 \qquad {}^3P_1 - \longrightarrow {}^3S_1 + E_1$$
$$^3S_1 \longrightarrow {}^3S_1 + M_1 \qquad {}^3P_2 - \longrightarrow {}^3S_1 + E_1$$
$$^1D_1 - \longrightarrow {}^3S_1 + E_1$$
$$^3P_0 - \longrightarrow {}^3S_1 + E_1$$

# 1 Introduction

The hadronic weak interaction manifests itself in parity-violating phenomena both in the two-nucleon system and in nuclei. A parity-violating signal is necessary to isolate experimentally the hadronic weak interaction (which does not conserve parity) from the much larger effects of the strong and electromagnetic interactions (which conserve parity). The weak interaction between nucleons in a nucleus was first observed in experiments on low energy polarized neutron capture in 1964 [2]. Since the pioneering experiments of Abov, parity-violating phenomena in nuclei have been extensively studied experimentally. Parity-violating alpha transitions, parity-violating circular $\gamma$-ray polarizations, parity-violating asymmetries from polarized nuclei, and most recently anapole moments of nuclear ground states have been observed and measured with good precision.

Although a theoretical framework (the weak meson-exchange potential) has been developed, the theoretical understanding of weak interactions in nuclei has not kept pace with experiment. In particular:

1. The weak couplings that give the spin, isospin, position, and momentum dependence of the potential have not yet been determined.

2. The validity of the description of the weak interaction in nuclei using a meson-exchange potential model has not been established.

3. A quantitative description of many measured parity-violating observables does not exist.

The determination of the weak meson-exchange couplings from measurements in nuclei has been difficult because the observables depend on the nuclear wave functions of the states involved in either transitions or moments. These wave functions can not be exactly calculated, except in few-nucleon systems. Measurements of parity violation have been made in the two-nucleon $pp$ system, where nuclear structure does not effect the interpretation. However, as discussed below, these observables depend upon the weak $\rho$ and $\omega$ couplings. In order to unambiguously determine the long-range $\Delta I = 1$ component of the weak interaction carried by the pion, measurements in the $np$ system are required.

The aim of the present proposal is to determine experimentally the most important of the couplings in the weak meson exchange potential, the weak pion-nucleon coupling $H_\pi^1$. As in the $pp$ system, there will be no ambiguity in the interpretation of the result arising from nuclear structure. We will measure the parity-violating directional correlation $A_\gamma$ between the spin direction of polarized neutrons and the $\gamma$-ray direction in the reaction $\vec{n} + p \rightarrow d + \gamma$. The observed asymmetry depends on only one of the couplings, the $\Delta I = 1$ pion coupling $H_\pi^1$, and therefore the lack of knowledge of the other couplings does not affect the determination of $H_\pi^1$. The weak exchange of the $\pi$, which is the lightest meson, contributes the longest-range component to the weak meson-exchange potential. In addition, the weak exchange of the pion contributes only to the $\Delta I = 1$ channel.

The determination of $H_\pi^1$ is important for several reasons:

1. A knowledge of $H_\pi^1$ is necessary to understand and interpret measurements of parity-violating observables in complex nuclei. For example, we discuss below a controversy concerning the interpretation of the measured anapole moment of $^{133}$Cs involving the value of $H_\pi^1$.

2. The knowledge of $H_\pi^1$ is an essential part of a program of measurements in two-nucleon systems to determine a complete set of the couplings in the weak meson-exchange potential. Such a program is both feasible, and partially complete.

3. In fact enough measurements in the two-nucleon system are possible to over constrain the weak meson-exchange couplings and test the validity of the meson exchange description of the weak force between nucleons. Once the weak meson-exchange potential has been established by measurements in two-nucleon systems, the interpretation of parity-violating phenomena in finite nuclei will be reduced to understanding the nuclear structure of the states involved.

4. A knowledge of $H_\pi^1$ will stimulate theoretical work to calculate $H_\pi^1$ starting from the standard-model description of weak interactions and a QCD description of the strong interactions.

## 1.1 Discussion of Mass Scales of the Weak Interactions

During the same period that parity-violating phenomena were being investigated in nuclei, there was rapid progress in experiments and theory studying weak interactions and decays of particles. As quarks were discovered and the electroweak theory was developed to explain leptonic and semi-leptonic weak processes and predict neutral weak currents, the parameters describing the weak interactions of quarks were fixed. $W^\pm$ and $Z^0$ boson production experiments at LEP and Fermilab verified that the strengths of $qqW^\pm$ and $qqZ^0$ weak couplings could be described by the standard model [3, 4, 5, 6, 7].

The challenge now is to connect the standard model description of the hadronic weak interaction across mass scales. These mass scales range from 100 GeV to the spacing of nuclear levels, 1 MeV. At the highest mass scale, that appropriate for the weak interactions of point-like leptons, QCD effects are small and the quark-quark weak interaction effects can be calculated. At lower mass scales, the appropriate degrees of freedom become composite and the role of the strong interaction becomes crucial. In order to put the problem of the weak interactions between nucleons in context we will briefly discuss these mass scales.

The largest mass scale is that of the mass of the gauge bosons of the weak interaction, the $W^\pm$ and the $Z^0$, $\approx$ 100 GeV. The standard model is thought to very accurately describe the weak interactions of point-like leptons; electrons, muons, taus, and their neutrinos. The leptons couple to their neutrinos with a universal $V - A$ weak coupling. The decay of a $\mu^-$

$$\mu^- \to e^- + \overline{\nu}_e + \nu_\mu$$

is typical of this class of decays and interactions. (See figure 1.) A small number of parameters, the Weinberg angle, the gauge boson, lepton, and neutrino masses, the neutrino mixing angles, and $\alpha$, must be determined experimentally.

For large momentum transfer (> 1 GeV) the weak interactions of quarks, such as dilepton production in $p\overline{p}$ scattering (see figure 2), is calculable using next-to-leading order QCD corrections to standard electroweak theory. The weak interactions of quarks are more complex than those of leptons. Linear combinations of quark fields, rather than the quark fields themselves, couple to the weak gauge bosons. In contrast to the lepton flavor, quark flavor is not conserved. In addition to the quark masses, the quark mixing angles (CKM matrix elements) must be determined from experiment.

The mass scale of bound systems of quarks such as nucleons and mesons is less than the QCD mass scale of $\Lambda \approx 1$ GeV. The simplest weak interactions of hadrons are their semi-leptonic decays. An example is neutron beta decay,

$$n \to p + e^- + \overline{\nu}_e,$$

# Contents


**1 Introduction** 3

1.1 Discussion of Mass Scales of the Weak Interactions . . . 4

1.2 Status of Our Knowledge of the Weak Meson-Nucleon Couplings . . . 8

1.2.1 Theoretical Estimates of the Sizes of the Weak Meson-Exchange Couplings . 8

1.2.2 What We Know from Experiments . . . 9

1.3 Strategy to Determine the Couplings from Two-Nucleon Experiments . . . 12

1.4 Calculations of $H_\pi^1$ . . . 13

1.5 Symmetry Considerations for $\vec{n} + p \to d + \gamma$ . . . 14

1.6 Role of the hadronic weak interaction in the study of the weak interaction . . . 15

1.7 Search for New Weak Neutral Gauge Bosons . . . 15

1.8 Summary . . . 15

**2 Advantages of LANSCE** 16

**3 Description of the Proposed Experiment** 17

3.1 Neutron Source and Optimization of the Experimental Configuration . . . 17

3.2 Neutron Polarizer . . . 24

3.2.1 Polarizing Super Mirrors . . . 24

3.2.2 Neutron Polarization with a $^3$He Spin Filter . . . 25

3.3 RF Spin Flipper . . . 31

3.4 Liquid Para-Hydrogen Target . . . 32

3.4.1 Target Vessel . . . 33

3.4.2 Ortho–Para-Hydrogen Conversion . . . 35

3.4.3 Cryocooler . . . 35

3.4.4 Vacuum system . . . 36

3.4.5 Hydrogen Safety . . . 36

3.4.6 Instrumentation . . . 37

3.5 Gamma Detector . . . 38

3.5.1 Cesium Iodide Scintillators . . . 38

3.5.2 Current Mode Signal . . . 40

3.5.3 Amplification of Photocathode Signal . . . 40

3.6 Detector Electronics . . . 41

3.6.1 Low-Noise Preamplifiers . . . 42

3.6.2 Sum and Difference Amplifiers . . . 42

3.7 Data Acquisition System . . . 42

3.7.1 VME-Based Data Acquisition Electronics . . . 44

3.7.2 PC-based Data Acquisition System (PC DAQ) . . . 44

3.7.3 Data Storage and Distribution . . . 45

3.8 Magnetic Guide Field . . . 45

4 Systematic Effects in the Experiment $\vec{n} + p \rightarrow d + \gamma$ 46
4.1 Statistical Errors . . . 46
4.2 Sources of Systematic Effects . . . 46
4.2.1 Systematic Errors of Instrumental Origin . . . 46
4.2.2 Systematic Errors from Interactions of the Neutron Spin . . . 48
4.2.3 Time-Dependent Effects . . . 51
4.3 Online Diagnostics . . . 53
4.3.1 Identification of Systematic Effects . . . 53
4.3.2 Target Diagnostics . . . 54
4.4 Auxiliary Measurements . . . 56

5 Progress to Date 57
5.1 Test Run . . . 57
5.1.1 Current-Mode Signal . . . 59
5.1.2 Electronic Noise . . . 60
5.1.3 Spectral Density . . . 61
5.1.4 Detector Sensitivity to Magnetic Fields . . . 61
5.2 Development of the Detector Electronics . . . 61
5.3 Computer Modeling . . . 63
5.3.1 Neutrons in the Liquid Para-Hydrogen Target . . . 63
5.3.2 Modeling of CsI Detector Array . . . 67
5.4 Neutron Guide and Shutter . . . 70

6 Progress Expected in the Near Future 72

7 Conclusion 72

A Budget and Manpower 74

B Schedule 78

C Personnel 79

D Publications and Presentations 84

$$^1S_0 \longrightarrow {}^3S_1 + M_1 \qquad {}^3P_1^- \longrightarrow {}^3S_1 + E_1$$

$$^3S_1 \longrightarrow {}^3S_1 + M_1 \qquad {}^3P_2^- \longrightarrow {}^3S_1 + E_1$$

$$^3P_1^- \longrightarrow {}^3S_1 + E_1$$

$$^3P_0^- \longrightarrow {}^3S_1 + E_1$$

# 1 Introduction

The hadronic weak interaction manifests itself in parity-violating phenomena both in the two-nucleon system and in nuclei. A parity-violating signal is necessary to isolate experimentally the hadronic weak interaction (which does not conserve parity) from the much larger effects of the strong and electromagnetic interactions (which conserve parity). The weak interaction between nucleons in a nucleus was first observed in experiments on low energy polarized neutron capture in 1964 [2]. Since the pioneering experiments of Abov, parity-violating phenomena in nuclei have been extensively studied experimentally. Parity-violating alpha transitions, parity-violating circular $\gamma$-ray polarizations, parity-violating asymmetries from polarized nuclei, and most recently anapole moments of nuclear ground states have been observed and measured with good precision.

Although a theoretical framework (the weak meson-exchange potential) has been developed, the theoretical understanding of weak interactions in nuclei has not kept pace with experiment. In particular:

1. The weak couplings that give the spin, isospin, position, and momentum dependence of the potential have not yet been determined.

2. The validity of the description of the weak interaction in nuclei using a meson-exchange potential model has not been established.

3. A quantitative description of many measured parity-violating observables does not exist.

The determination of the weak meson-exchange couplings from measurements in nuclei has been difficult because the observables depend on the nuclear wave functions of the states involved in either transitions or moments. These wave functions can not be exactly calculated, except in few-nucleon systems. Measurements of parity violation have been made in the two-nucleon $pp$ system, where nuclear structure does not effect the interpretation. However, as discussed below, these observables depend upon the weak $\rho$ and $\omega$ couplings. In order to unambiguously determine the long-range $\Delta I = 1$ component of the weak interaction carried by the pion, measurements in the $np$ system are required.

The aim of the present proposal is to determine experimentally the most important of the couplings in the weak meson exchange potential, the weak pion-nucleon coupling $H_\pi^1$. As in the $pp$ system, there will be no ambiguity in the interpretation of the result arising from nuclear structure. We will measure the parity-violating directional correlation $A_\gamma$ between the spin direction of polarized neutrons and the $\gamma$-ray direction in the reaction $\vec{n} + p \rightarrow d + \gamma$. The observed asymmetry depends on only one of the couplings, the $\Delta I = 1$ pion coupling $H_\pi^1$, and therefore the lack of knowledge of the other couplings does not affect the determination of $H_\pi^1$. The weak exchange of the $\pi$, which is the lightest meson, contributes the longest-range component to the weak meson-exchange potential. In addition, the weak exchange of the pion contributes only to the $\Delta I = 1$ channel.

The determination of $H_\pi^1$ is important for several reasons:

1. A knowledge of $H_\pi^1$ is necessary to understand and interpret measurements of parity-violating observables in complex nuclei. For example, we discuss below a controversy concerning the interpretation of the measured anapole moment of $^{133}$Cs involving the value of $H_\pi^1$.

2. The knowledge of $H_\pi^1$ is an essential part of a program of measurements in two-nucleon systems to determine a complete set of the couplings in the weak meson-exchange potential. Such a program is both feasible, and partially complete.

3. In fact enough measurements in the two-nucleon system are possible to over constrain the weak meson-exchange couplings and test the validity of the meson exchange description of the weak force between nucleons. Once the weak meson-exchange potential has been established by measurements in two-nucleon systems, the interpretation of parity-violating phenomena in finite nuclei will be reduced to understanding the nuclear structure of the states involved.

4. A knowledge of $H_\pi^1$ will stimulate theoretical work to calculate $H_\pi^1$ starting from the standard-model description of weak interactions and a QCD description of the strong interactions.

## 1.1 Discussion of Mass Scales of the Weak Interactions

During the same period that parity-violating phenomena were being investigated in nuclei, there was rapid progress in experiments and theory studying weak interactions and decays of particles. As quarks were discovered and the electroweak theory was developed to explain leptonic and semi-leptonic weak processes and predict neutral weak currents, the parameters describing the weak interactions of quarks were fixed. $W^\pm$ and $Z^0$ boson production experiments at LEP and Fermilab verified that the strengths of $qqW^\pm$ and $qqZ^0$ weak couplings could be described by the standard model [3, 4, 5, 6, 7].

The challenge now is to connect the standard model description of the hadronic weak interaction across mass scales. These mass scales range from 100 GeV to the spacing of nuclear levels, 1 MeV. At the highest mass scale, that appropriate for the weak interactions of point-like leptons, QCD effects are small and the quark-quark weak interaction effects can be calculated. At lower mass scales, the appropriate degrees of freedom become composite and the role of the strong interaction becomes crucial. In order to put the problem of the weak interactions between nucleons in context we will briefly discuss these mass scales.

The largest mass scale is that of the mass of the gauge bosons of the weak interaction, the $W^\pm$ and the $Z^0$, $\approx$ 100 GeV. The standard model is thought to very accurately describe the weak interactions of point-like leptons; electrons, muons, taus, and their neutrinos. The leptons couple to their neutrinos with a universal $V - A$ weak coupling. The decay of a $\mu^-$

$$\mu^- \rightarrow e^- + \overline{\nu}_e + \nu_\mu$$

is typical of this class of decays and interactions. (See figure 1.) A small number of parameters, the Weinberg angle, the gauge boson, lepton, and neutrino masses, the neutrino mixing angles, and $\alpha$, must be determined experimentally.

For large momentum transfer (> 1 GeV) the weak interactions of quarks, such as dilepton production in $p\overline{p}$ scattering (see figure 2), is calculable using next-to-leading order QCD corrections to standard electroweak theory. The weak interactions of quarks are more complex than those of leptons. Linear combinations of quark fields, rather than the quark fields themselves, couple to the weak gauge bosons. In contrast to the lepton flavor, quark flavor is not conserved. In addition to the quark masses, the quark mixing angles (CKM matrix elements) must be determined from experiment.

The mass scale of bound systems of quarks such as nucleons and mesons is less than the QCD mass scale of $\Lambda \approx 1$ GeV. The simplest weak interactions of hadrons are their semi-leptonic decays. An example is neutron beta decay,

$$n \rightarrow p + e^- + \overline{\nu}_e,$$

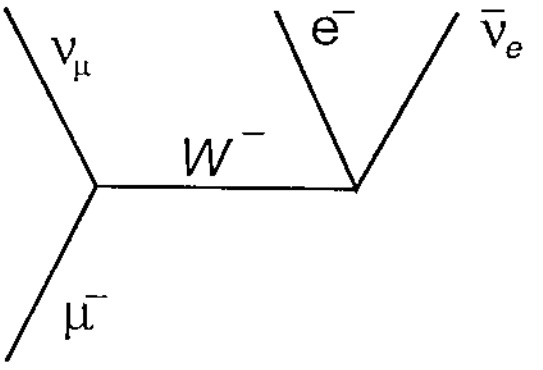


Figure 1: Decay of the $\mu^-$ through the leptonic weak interaction.

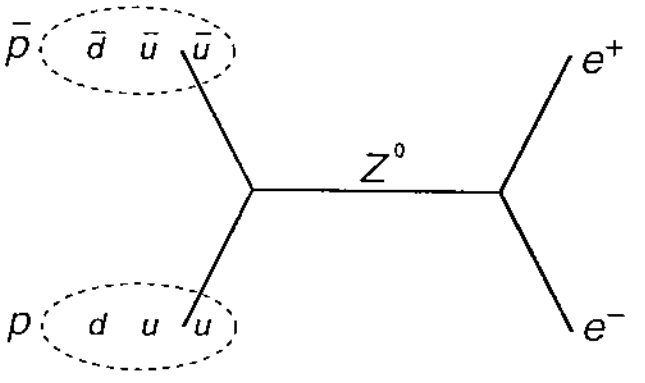


Figure 2: Dilepton production in $p\bar{p}$ scattering.

shown in figure 3. The strong interactions of quarks, through gluon exchange, modify semi-leptonic decay rates from the values that would be expected in their absence. For example, the magnitude of the axial vector coupling constant $G_A$ in neutron beta decay is 30% larger than the vector coupling constant $G_V$.

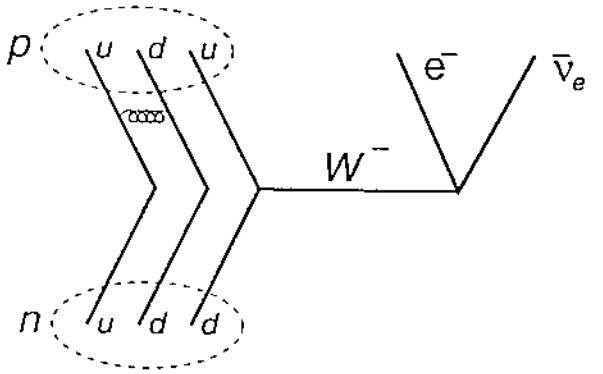


Figure 3: Decay of the neutron through the semi-leptonic weak interaction.

Just like purely leptonic and semi-leptonic weak interactions, purely hadronic weak interaction between nucleons can be mediated by the exchange of the $W^{\pm}$ and $Z^0$ bosons. At momentum transfers typical of nucleon-nucleon or nuclear interactions, $\approx 300$ MeV, the appropriate degrees of freedom are meson and nucleons. The range of the $W^{\pm}$ and $Z^0$ is $\approx 0.02$ fm, much shorter than the distance between nucleons. The hard-core repulsion in the $NN$ interaction keeps the nucleons much farther apart than the range of the weak gauge bosons. The long-range weak force between nucleons is mediated by the exchange of light mesons. As shown in figure 4, a weak gauge boson, is emitted by a quark, travels a short distance, and changes into a $\pi$, $\rho$, or $\omega$, which then couples strongly to another nucleon. As in the case of semi-leptonic decays, the coupling strengths are modified by strong interactions of the bound quarks.

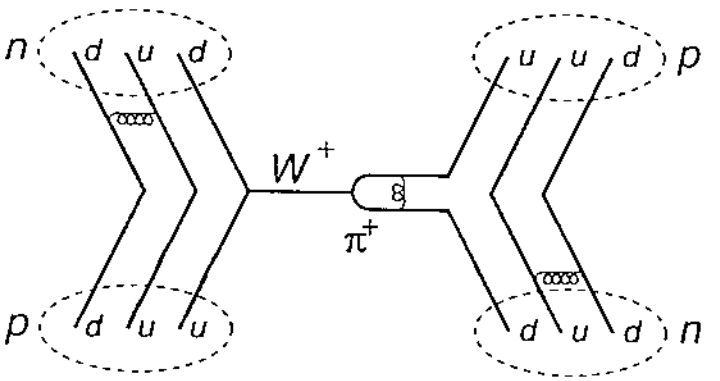


Figure 4: Neutron-proton scattering, mediated by the hadronic weak interaction.

The above description of parity-violating phenomena in nuclei has taken as its starting point the weak meson-exchange potential model described by figure 5. The degrees of freedom are nucleons and mesons. The exchanged weak gauge boson has been collapsed into a weak meson-nucleon vertex. The weak interaction can change isospin and therefore isospin is not conserved at the weak vertex. The other vertex describes the the strong interaction of mesons and nucleons and the couplings are known experimentally. Because QCD has not been solved for bound systems, the weak meson-nucleon couplings $H_\mu^{\Delta I}$ must be determined from experiment. The weak meson-exchange potential $V_{pnc}$ has the form

$$V_{pnc} = \sum_{\mu=\pi,\rho,\omega} \sum_{\Delta I=0,1,2} H_\mu^{\Delta I} V_\mu^{\Delta I} \tag{1}$$

where $V_{pnc}$ is a linear combination of terms each involving the exchange of a $\pi$, $\rho$, or $\omega$ meson with a second index describing the isospin exchanged in the weak interaction. For example the $\Delta I = 1$ pion potential has the following form:

$$V_\pi^1 = \frac{i}{m} [\vec{\tau}_1 \times \vec{\tau}_2]_z (\vec{\sigma}_1 + \vec{\sigma}_2) \cdot \vec{u}_\pi(\vec{r}), \tag{2}$$

where $m$ is the nucleon mass,

$$\vec{u}_\pi(\vec{r}) = \left[\vec{p}, \frac{e^{-m_\pi r}}{4\pi r}\right], \tag{3}$$

$m_\pi$ is the pion mass, $\vec{r} = \vec{r}_1 - \vec{r}_2$, and $\vec{p} = \vec{p}_1 - \vec{p}_2$. The Yukawa function in $\vec{u}_\pi(\vec{r})$ (and the weak potentials for the other mesons) gives the dependence of $V_\pi^1$ on the separation of the two interacting nucleons. The range of $V_\pi^1$ is longer than that of the other weak meson potentials.

The parity-violating nucleon-nucleon interaction is much weaker than the strong nucleon-nucleon interaction. Theories of parity violating phenomena in nuclei start with solutions of the strong, parity-conserving, nuclear Hamiltonian $\psi$ and admix parity-odd components $\phi$ treating the two-body weak meson-exchange potential as a perturbation.

$$\psi' = \psi + \frac{\langle\phi|V_{pnc}|\psi\rangle}{\Delta E}\phi. \tag{4}$$

An observable such as a nuclear anapole moment $a$ can be expressed as a matrix element of the corresponding operator:

$$a = \frac{\pi e \mu}{m} \langle\psi'|\vec{r} \times \vec{\sigma}|\psi'\rangle, \tag{5}$$

where $e$ is the quantum of charge and $\mu$ is the magnetic moment of the unpaired nucleon. If the observable involves a transition between states, the initial and final states would be different. It is evident that each parity-violating observable is given by a linear combination of the weak meson-nucleon couplings times matrix elements of operators between nuclear states. For the two-body system the wave functions are known, the matrix elements can be reliably calculated, and the relationship between observables and the couplings is unambiguous. For more than a few bodies the nuclear wave functions can not be exactly calculated and the expressions for parity-violating observables are uncertain for two reasons: the couplings are not known and the nuclear matrix elements can not be reliably calculated.

The strategy of the present proposal is to overcome the problem of imperfect knowledge of the nuclear wave function by experimentally determining a parity-violating observable in the two-body system. We propose to measure the directional asymmetry of the direction of emission of the $\gamma$-ray

has recently revised the "reasonable range" for $H_\pi^1$ [9]. DDH considered exchanges of the three lightest mesons, $\pi$, $\rho$, and $\omega$. There are seven possible couplings that are labeled according to the meson exchanged and the isospin exchanged $\Delta I$ at the vertex. Adelberger and Haxton [1] give expressions for parity-violating observables in their review.

| Exchanged Meson | Coupling | $\Delta I$ | "Best Value" ($10^{-6}$) | "Reasonable Range" ($10^{-6}$) |
|---|---|---|---|---|
| $\pi$ | $H_\pi^1$ | 1 | 1.08 | 0.0–2.71 |
| $\rho$ | $H_\rho^0$ | 0 | 1.59 | −1.59–4.29 |
| $\rho$ | $H_\rho^1$ | 1 | 0.03 | 0.0–0.053 |
| $\rho$ | $H_\rho^2$ | 2 | 1.33 | −1.06–1.54 |
| $\rho$ | $H'^1_\rho$ | 1 | 0.00 | none |
| $\omega$ | $H_\omega^0$ | 0 | 0.80 | −2.39–4.29 |
| $\omega$ | $H_\omega^1$ | 1 | 0.48 | 0.32–0.80 |

Table 1: Estimated weak meson-nucleon couplings from ref. [1].

It is evident that if the couplings $H_\rho^1$ and $H'^1_\rho$ satisfy the bounds given in table 1, they will play a negligible role in determining the outcomes of experiments. In what follows we concentrate on the remaining 5 couplings.

### 1.2.2 What We Know from Experiments

**Experiments in the *pp* System** An extensive program of high-quality experiments has been carried out to measure the parity-violating longitudinal asymmetry $A_z$ in the scattering of polarized protons from unpolarized protons at 15 and 45 MeV. These experiments show the predicted energy dependence of the longitudinal asymmetry. The experiments determine a linear combination of weak couplings, for example at 45 MeV $A_z$ is given by

$$A_z = -0.053\left(H_\rho^0 + H_\rho^2/\sqrt{6}\right) - 0.016\left(H_\omega^0 + H_\omega^1\right), \tag{6}$$

to an accuracy of 10%.

**Experiments in the *np* System** Measurements have been made in *np* capture of both the directional asymmetry $A_\gamma$ and circular polarization $P_\gamma$ of the emitted $\gamma$-rays. Both experiments were statistically limited, and yielded null results. In the first case, Caviagnac, *et al.* [10] report a value of $A_\gamma = 0.6 \pm 2.1 \times 10^{-7}$, which gives for the $\Delta I = 1$ weak pion coupling $H_\pi^1 = -1.3 \pm 4.7 \times 10^{-6}$ (see equation 20). In the second case, Knyaz'kov, *et al.* [11] report a value of $P_\gamma = 1.8 \pm 1.8 \times 10^{-7}$, which gives for the combination of the $\Delta I = 0$ and 2 weak rho couplings $H_\rho^0 + 2H_\rho^2/\sqrt{6} = 8.2 \pm 8.2 \times 10^{-6}$ (see equation 12). The inverse reaction, deuteron photo-disintegration by circularly polarized $\gamma$-rays, has been measured by Earle, *et al.* [12], who also report a null result. These experimental limits are less stringent than the "reasonable ranges" given in table 1. Clearly, experiments with improved statistical precision are required.

**Measurement of $P_\gamma$ from $^{18}$F and its Interpretation** The determination of the weak meson-nucleon exchange couplings from experimental measurements in nuclei are discussed in the review by Adelberger and Haxton[1]. There are substantial uncertainties in interpreting most experiments in nuclei because one cannot make reliable *ab initio* calculations of the amplitudes of the weak meson-nucleon exchange potential operators. The circular polarization $P_\gamma$ of the 1081 keV transition in $^{18}$F is an exception to this unfortunate situation because the matrix elements needed to extract a value for $H_\pi^1$ from experiments can be measured. The circular polarization of a $\Delta I = 1$ parity forbidden gamma transition in $^{18}$F has been measured in five different and internally consistent experiments (references given in [1]). To a good approximation the circular polarization is due to the parity-violating mixing between the $J = 0$, $I = 0$ parity-odd level ($|-\rangle$) in $^{18}$F and the nearly degenerate $J = 0$, even-parity, $I = 1$ level ($|+\rangle$). The circular polarization is given by:

$$P_\gamma = \frac{2}{\Delta E}\frac{\langle +|V_{pnc}|-\rangle\langle gs|M1|+\rangle}{\langle gs|E1|-\rangle}. \tag{7}$$

The magnitudes of the $M1$ and $E1$ transition amplitudes and the energy splitting $\Delta E = 39$ keV between the levels are known experimentally. Bennet, Lowry, and Krien [13] and Haxton [14] pointed out that the unknown amplitude, $\langle +|V_{pnc}|-\rangle$, could be related to the lifetime of the first forbidden beta decay between isobaric analog states of $|+\rangle$ and $|-\rangle$ in $^{18}$Ne. For beta transitions between opposite parity $J = 0$ levels, spin and parity selection rules exclude all but two of the six possible transition amplitudes. One of these vanishes in the long wavelength limit leaving only the $M_{00}^5$ amplitude. Haxton uses PCAC, current algebra, and the approximation that the neutron and proton densities are the same for the $A = 18$ system to argue that the two-body part of $M_{00}^5$ renormalizes the one-body part and that the operator for the weak nucleon-nucleon potential due to pion exchange is to within a known constant an isospin rotation of the operator for $M_{00}^5$. Haxton estimates the contributions of heavy mesons as a 5% correction to the pion term. Since the experimental value of the asymmetry, $P_\gamma = 8 \pm 39 \times 10^{-5}$, is consistent with zero, an upper limit for $H_\pi^1$ results. Adelberger and Haxton find $H_\pi^1 < 0.35 \times 10^{-6}$. This value is a fraction of the DDH "best" value and is an order of magnitude smaller than the "reasonable range". This result has been interpreted as evidence for (unexpected) suppression of quark-quark neutral currents. Haxton's arguments, outlined above, appear sound. The comparison of $H_\pi^1$ from $^{18}$F and $H_\pi^1$ from $\vec{n} + p \rightarrow d + \gamma$ will test the applicability of the weak meson-exchange potential to weak phenomena in $A > 3$ nuclei.

**Measurements of the Anapole Moments $^{133}$Cs and $^{205}$Tl and their Interpretation** Recently, the anapole moments of nuclear ground states have been observed using laser spectroscopy on atomic beams. These measurements have observed, for the first time, a static moment of a nucleus that is forbidden by parity. Although in its infancy, the experimental study of nuclear anapole moments is potentially important to the understanding of the weak interaction in nuclei because nuclear anapole moments can be measured in many nuclei and their systematic behavior established. Knowledge of systematics can then be used to check the correctness of the models used to determine the nuclear wave functions.

The anapole moment operator [15] is a parity-odd rank one tensor and is given by

$$\vec{a} = -\pi \int r^2 \vec{j}(r)\, d^3r, \tag{8}$$

where $\vec{j}(r)$ is the electromagnetic current density operator. The anapole moment has an expectation

value of zero for states of definite parity. The size of the anapole moment is given by the dimensionless constant $\kappa_a$, whose value is thought to be theoretically stable for three reasons:

1. The anapole moment of a nuclear state is a diagonal matrix element, in contrast to a transition matrix element.

2. The nuclear wave function can be constrained by the measured magnetic moment of the state. The single-particle estimate is $\mu_{sp} = 1.72$ for $^{133}$Cs and $\mu_{sp} = 2.79$ for $^{205}$Tl (see, for example, [16]). By comparison, the experimental values are $\mu_{exp} = 2.58$ and $\mu_{exp} = 1.64$, respectively. The rough agreement between the single-particle estimates and experimental values of the magnetic moments justifies the theoretical approach to anapole moments of starting from single-particle estimates and then adding many-body effects as corrections. Information on the spatial distribution of the electromagnetic current can be obtained from the magnetic hyperfine anomaly. This information can be used to constrain the wave function.

3. The contribution to anapole moment of the spin of the odd proton (neutron) can be estimated analytically and gives results close to those from full many-body calculations[1] [17].

The estimate of the one-body part of the anapole moment is similar to the calculation of the contribution of the spin of the unpaired nucleon to the magnetic moment of a nucleus. The analytical estimate [18] gives a value in rough agreement with detailed nuclear structure calculations by Haxton [19], Haxton, Henley, and Musolf [20], Flambaum and Murray [21], and Dmitriev and Telitsin [17]. The latter is the most recent calculation and includes the effects of spin, spin-orbit, convection, and contact currents, many-body corrections, and RPA re-normalization of the weak interaction addition to the single-particle weak interaction.

The non-zero measurement of the anapole moment of $^{133}$Cs [22] has been analyzed by Flambaum and Murray [21] to extract a value for $H^1_\pi$. Their result, $H^1_\pi = 2.26 \pm 0.50(\text{expt}) \pm 0.83(\text{theor}) \times 10^{-6}$ is a factor of two larger than the DDH value and a factor of *seven* larger than the upper limit set by the $^{18}$F experiments. Their analysis, however, is controversial for two reasons [23]. First, the $^{133}$Cs anapole moment is almost as sensitive to $H^1_\rho$ as to $H^1_\pi$. Wilburn and Bowman find

$$\kappa_a \approx 1.05 \times 10^5 \left(H^1_\pi + 0.69 H^0_\rho\right). \tag{9}$$

Because of this sensitivity, and because of the lack of model-independent constraints on $H^0_\rho$, it is possible to extract values of the two couplings that agree with both experiments. Secondly, the result from $^{133}$Cs are inconsistent with an earlier null measurement of the anapole moment of $^{205}$Tl [24]. The situation is summarized in figure 6. This result suggests that nuclear structure effects that are not included in the theory may be important in interpreting the measurements, assuming both measurements are correct.

The present controversy concerning the interpretation of measured nuclear anapole moments highlights the need to determine the weak couplings from experiments in few-nucleon systems whose interpretation is free from uncertainties in nuclear structure and demonstrates the nuclear physics that can be learned. If the weak meson-nucleon couplings were known, the present controversy could be more definitively addressed. One would calculate the values of the anapole moments using the measured values of the couplings from few-nucleon experiments; if the measured values of the anapole moments disagreed with these predictions, the problem would lie with the measurements, the nuclear theory, or the applicability of the meson-exchange model to nuclei.

[1] Dmitriev and Telitsin find that a naive harmonic oscillator model gives results that agree with their full calculation to within 10%.

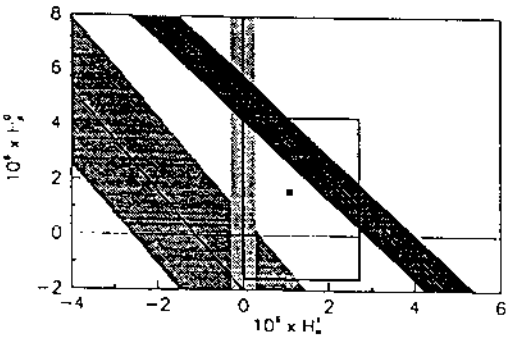


Figure 6: Weak coupling constants $H_\pi^1$ and $H_\rho^0$ extracted from the $^{18}$F (light band), $^{205}$Tl (medium band), and $^{133}$Cs (dark band) experiments. Also shown are the DDH "best" values (square) and "reasonable range" (box).

## 1.3 Strategy to Determine the Couplings from Two-Nucleon Experiments

The purpose of the present proposal is to determine the most important coupling, $H_\pi^1$. This determination of $H_\pi^1$, free from any uncertainties arising from nuclear structure, will be the cornerstone of any effort to determine a complete set of couplings. In the expressions for most experimental observables, $H_\pi^1$ occurs in combination with others. It is therefore highly desirable to develop an experimental program to determine the other couplings.

As discussed in section 1.2.2, the PSI measurement of $A_z$ in $pp$ scattering at 45 MeV is given by a linear combination of $H_\rho^0$, $H_\rho^2$, $H_\omega^0$, and $H_\omega^1$:

$$A_z = -0.053\left(H_\rho^0 + H_\rho^2/\sqrt{6}\right) - 0.016\left(H_\omega^0 + H_\omega^1\right). \tag{10}$$

An experiment in progress at TRIUMF [25] to measure $A_z$ at 221 MeV is sensitive to only the $\rho$ couplings:

$$A_z = 0.028\left(H_\rho^0 + H_\rho^2/\sqrt{6}\right). \tag{11}$$

The low energy $pp$ experiment and the TRIUMF experiment will determine the linear combination of $\omega$ couplings $H_\omega^0 + H_\omega^1$ and the linear combination of $\rho$ couplings $H_\rho^0 + H_\rho^2/\sqrt{6}$. One further experiment is necessary to separate the two $\rho$ couplings.

The problem of separately determining the weak $\rho$ couplings could be resolved by measuring the circular polarization $P_\gamma$ of the gammas emitted in the $\vec{n} + p \to d + \gamma$ reaction. This observable is primarily sensitive to the $\Delta I = 0$ and 2 $\rho$ couplings [1]:

$$P_\gamma = 0.022H_\rho^0 + 0.043H_\rho^2/\sqrt{6} - 0.002H_\omega^0. \tag{12}$$

The combination of this measurement and the TRIUMF $pp$ measurement would then independently determine $H_\rho^0$ and $H_\rho^2$. In practice, it is experimentally easier to measure the inverse reaction, the directional asymmetry in the photo-disintegration of the deuteron by circularly polarized photons, due to the low efficiency of $\gamma$-ray polarization analyzers. As in the case of $A_\gamma$, existing measurements

of $P_\gamma$ (or of the inverse reaction) [26, 11, 12] are not of sufficient precision to accomplish this task. With the availability of very intense gamma beams from Compton back-scattering using free electron lasers [27], a more precise measurement of the deuteron photo-disintegration asymmetry is possible and should be pursued.

Finally, there is another observable in the $np$ system that is primarily sensitive to $H_\pi^1$: the parity-violating spin rotation of transversely polarized neutrons in a liquid para-hydrogen target. There is a theoretical calculation for the low-energy neutron spin rotation angle $\phi_{PNC}$ per unit length in para-hydrogen [28]

$$\phi_{PNC} = -1.31H_\pi^1 - 0.23H_\rho^0 - 0.25H_\rho^2 - 0.23H_\omega^0, \tag{13}$$

in units of radians per meter, which implies that this observable is also primarily sensitive to $H_\pi^1$. An experimental sensitivity of about $2 \times 10^{-6}$ radians per meter would be required to see this effect for the DDH value of $H_\pi^1$. The sensitivity goal for a similar experiment in progress to search for parity violating neutron spin rotation in helium is $1 \times 10^{-7}$ radians per meter [29]. An experiment to measure the longitudinal asymmetry $A_z$ in $np$ scattering at neutron energies of tens of MeV is also possible. This observable is sensitive to $H_\pi^1$ and other couplings. A theoretical calculation of this observable is in progress [30]. With the addition of these two experiments, we begin to be able to over constrain the weak couplings and test the internal consistency of the meson exchange picture of the weak $NN$ interaction.

## 1.4 Calculations of $H_\pi^1$

The estimate of $H_\pi^1$ from the quark model and weak SU(6) symmetry have been discussed above. The revised estimate of the "reasonable range" by Desplanques is: $0 < H_\pi^1 < 0.6 \times 10^{-6}$ down from $0 < H_\pi^1 < 1.1 \times 10^{-6}$ by Desplanques, Donoghue, and Holstein. Recently, Henley, Hwang, and Kisslinger [31] have carried out QCD sum rule calculations of $H_\pi^1$. These calculations include the effects of gluon exchange that are absent in earlier quark model calculations. Henley *et al.* make the approximation that there are no strange quarks in the nucleon or charged pion. There are therefore no contributions to $H_\pi^1$ from $W^\pm$ exchange [32]. In any case, the contributions of charged currents would be Cabbibo suppressed if strange quarks were included. The calculation of Henley *et al.* adds $Z^0$ exchange to the diagrams involved in the strong interaction of the pion and the nucleon. Non-perturbative effects are described by the polarizability of a pion condensate in both the calculation of the strong pion-nucleon-nucleon coupling, $g_{\pi NN}$, and the weak meson-nucleon-nucleon coupling, $H_\pi^1$. Henley *et al.* fit the polarizability of the pion condensate to the experimental value of $g_{\pi NN}$. This procedure leads to a prediction of a small value of $H_\pi^1 = 0.5 \times 10^{-7}$, about half the error expected from the proposed measurement.

Kaplan and Savage present a contrary view concerning the role of strangeness [33]. They estimate $H_\pi^1$ and other parity-violating couplings in the framework of pion chiral perturbation theory. They explicitly consider the strange and anti-strange sea quark component of the nucleon wave function. Kaplan and Savage estimate that the contribution of strange components of the nucleon to $H_\pi^1$ may be as large as $1.4 \times 10^{-6}$. They argue multi-pion exchange may invalidate the conclusion that the $^{18}$F experiment can be interpreted as a measurement of $H_\pi^1$. Kaplan and Savage give a large theoretical uncertainty in these estimates. The quark model and QCD calculations favor small values of $H_\pi^1$. The chiral perturbation theory estimates suggest the possibility that $H_\pi^1$ may be large due to strangeness, but the uncertainty in these estimates is large. An experiment that provides a statistically accurate value of $H_\pi^1$ with small systematic and theoretical errors will challenge theories

that attempt to evaluate $H_\pi^1$ and will stimulate work in the calculation of the modification of weak interactions between quarks in the non-perturbative regime.

## 1.5 Symmetry Considerations for $\vec{n} + p \to d + \gamma$

It is worth understanding the reasons why the parity-violating gamma asymmetry, $A_\gamma$, in the reaction $\vec{n}+p \to d+\gamma$ is primarily sensitive to only the $\Delta I = 1$ component of the weak interaction. First of all, due to the large size of the deuteron only the longest-range components of the $NN$ interaction (due to $\pi$ and $\rho$ exchange) are important in this reaction. From the non-relativistic weak $NN$ potential, weak $\pi$ exchange is $\Delta I = 1$ and weak $\rho$ exchange is mainly $\Delta I = 0$ and $\Delta I = 2$.

Now consider the possible electromagnetic transitions in the $\vec{n} + p \to d + \gamma$ reaction. For low-energy neutrons, we will consider only $L = 0$ and $L = 1$ capture and reaction channels. Without parity violation, the channels for the initial state are $\left|{}^1S_0, I = 1\right\rangle_i$ and $\left|{}^3S_1, I = 0\right\rangle_i$ and the final state channel for the $(J^\pi, I) = (1^+, 0)$ deuteron is $\left|{}^3S_1, I = 0\right\rangle_D$ (ignoring the small tensor component in the deuteron). The weak interaction mixes in the following $L = 1$ components to the singlet and triplet $S$-waves in both the initial and final states:

$$\left|{}^1S_0, I = 1\right\rangle_i \longrightarrow \left|{}^1S_0, I = 1\right\rangle_i + f_0 \left|{}^3P_0, I = 1\right\rangle_i, \tag{14}$$

$$\left|{}^3S_1, I = 0\right\rangle_i \longrightarrow \left|{}^3S_1, I = 0\right\rangle_i + g_0 \left|{}^1P_1, I = 0\right\rangle_i + g_1 \left|{}^3P_1, I = 1\right\rangle_i, \tag{15}$$

$$\left|{}^3S_1, I = 0\right\rangle_D \longrightarrow \left|{}^3S_1, I = 0\right\rangle_D + h_0 \left|{}^1P_1, I = 0\right\rangle_D + h_1 \left|{}^3P_1, I = 1\right\rangle_D, \tag{16}$$

where the $f_I$, $g_I$ and $h_I$ terms are the amplitudes of the small weak interaction-induced admixtures with isospin change $I$. If one now writes down the matrix elements of the electromagnetic interaction, keeping only the lowest order multipoles consistent with parity conservation in the electromagnetic interaction and with isospin selection rules that forbid $E1$ transitions in self-conjugate nuclei like the deuteron, one obtains the parity conserving term $\langle M1 | \langle {}^3S_1, I = 0 |_D H_{em} | {}^1S_0, I = 1 \rangle$ and the parity violating terms

$$f_0 \langle E1 | \langle {}^3S_1, I = 0 |_D H_{em} | {}^3P_0, I = 1 \rangle, \tag{17}$$

$$g_1 \langle E1 | \langle {}^3S_1, I = 0 |_D H_{em} | {}^3P_1, I = 1 \rangle, \tag{18}$$

$$h_1 \langle E1 | \langle {}^3P_1, I = 1 |_D H_{em} | {}^3S_1, I = 0 \rangle. \tag{19}$$

Finally, since a gamma asymmetry cannot be produced from a $J = 0$ initial state, we are left with only a $\Delta I = 1$ contribution to parity violation in the gamma asymmetry. There are small corrections to this argument from isospin violation, higher-order multipole contributions, relativistic effects etc. but the main result survives a more exact treatment. This result was first obtained by Danilov [34].

There are two calculations of $A_\gamma$ as a function of the weak couplings. Adelberger and Haxton [1] find:

$$A_\gamma = -0.045 \left( H_\pi^1 - 0.02 H_\rho^1 + 0.02 H_\omega^1 + 0.04 H'^1_\rho \right). \tag{20}$$

The contributions of the non-pion couplings are estimated by taking the DDH upper limits $H_\rho^1 = 5 \times 10^{-8}$ and $H_\omega^1 = 8 \times 10^{-7}$. Desplanques and Missimer, who use $H_\pi^1$ and weak nucleon-nucleon amplitudes $X$ to parameterize the weak nucleon-nucleon interaction [35], find:

$$A_\gamma = -0.045 \left( H_\pi^1 + 0.11 X_{pn}^+ - 0.11 X_{pn}^- \right). \tag{21}$$

The $X$'s are linear combinations of the $\Delta I = 1$ meson exchange couplings other than $H_\pi^1$. These calculations of $A_\gamma$ agree on the coefficient of $H_\pi^1$ and both find the contributions from other mesons to be small. An accurate measurement of $A_\gamma$ is therefore an accurate measurement of $H_\pi^1$.

## 1.6 Role of the hadronic weak interaction in the study of the weak interaction

The study of parity violation in nuclei has played an important role in the development of our understanding of the weak interaction. The current-current hypothesis for the form of the weak interaction implies that parity admixture in nuclear wave functions would be first order in the Fermi coupling $G_F$, while the four-Fermion form of the weak interaction implies second-order admixtures. The observation of circular polarization in a gamma transition in $^{181}$Ta, $P_\gamma \sim 10^{-7}$, by Lobashov, *et al.* [36, 37] gave strong support to the current-current hypothesis.

## 1.7 Search for New Weak Neutral Gauge Bosons

As the search for weak neutral currents was being pursued, it was recognized that the hadronic weak interaction might be a good place to search for and study weak neutral currents. In contrast to charged currents the contributions of weak neutral currents to the $\Delta I = 1$ hadronic weak interaction are not Cabibbo suppressed. The $\Delta I = 1$ pion coupling might be strongly influenced by weak neutral currents; in the language of the standard model $Z^0$ exchange. As discussed above, the $qqZ^0$ has been measured in large momentum transfer experiments. The existence of the $qqZ^0$ coupling implies the existence of a weak neutral current contribution to the weak nucleon-nucleon interaction, according to figure 3. The standard model is widely believed to be incomplete. If in addition to the $Z^0$ of the standard model, there exist other gauge bosons that couple to quarks and do not decay into leptons, these additional $Z^0$'s would also contribute to $H_\pi^1$, but would not be observed in other processes. The role of the hadronic weak interaction as a direct probe of weak neutral currents is emphasized by Adelberger and Haxton [1]. However, we note that, the bound QCD problem has not yet been solved and there is considerable uncertainties in calculations of $H_\pi^1$ from the weak neutral current of the standard model. Until such calculations are possible only very large effects of additional $Z^0$'s will be detectable in $H_\pi^1$.

## 1.8 Summary

The experiment to measure the directional asymmetry of gammas $A_\gamma$ in $\vec{n} + p \rightarrow d + \gamma$ and extract a value of $H_\pi^1$ is of great interest for the following reasons:

1. We will show in section 3 that the experiment will measure the asymmetry with a statistical error of $0.5 \times 10^{-8}$ and a negligible systematic error. A measurement of $A_\gamma$ to this precision allows interesting conclusions to be drawn concerning $H_\pi^1$.

2. There is no nuclear structure uncertainty in the relationship between $H_\pi^1$ and the asymmetry. The uncertainty in the extracted value of $H_\pi^1$ will be small, 10% of the DDH theoretical estimate, given in table 1. There will be no uncertainties due to experimental systematic errors or nuclear structure. To a good approximation the asymmetry depends only on $H_\pi^1$.

3. An unambiguous value for $H_\pi^1$ will test theories of the weak interaction of hadrons in the non-perturbative regime and stimulate theoretical work in this area.

4. An unambiguous measurement will settle any controversy raised by the $^{133}$Cs anapole moment and $^{18}$F circular polarization results and their interpretation. The comparison of $H_\pi^1$ from $\vec{n} + p \rightarrow d + \gamma$ and $H_\pi^1$ from $^{18}$F will test the applicability of the meson-exchange potential to $A > 3$ systems.

5. The determination of $H_\pi^1$ is the cornerstone of a feasible and partially complete program to over-constrain the weak $NN$ couplings from parity-violating phenomena in the exactly calculable two-nucleon system.

6. The study of parity violation in the nucleon-nucleon interactions remains the only experimental means to directly study the weak neutral current interaction between quarks.

# 2 Advantages of LANSCE

LANSCE is uniquely suited as a site for this measurement. LANSCE has the only intense pulsed neutron source available for nuclear physics research and Los Alamos has a scientific staff that is unusually well qualified for this experiment.

When the upgrades currently in progress are complete, the Lujan Center spallation source will be the highest flux pulsed source in the world, equaling ISIS in average flux and exceeding it in peak flux. As noted throughout this proposal, there are compelling reasons for carrying out this experiment at a pulsed neutron source. Specific examples include:

- the pulsed nature of the beam provides neutron time-of-flight information, allowing determination of the neutron energy,
- systematic effects can be studied by their differing time-of-flight behaviors,
- the pulsed beam allows the use of a resonant RF spin flipper, eliminating the $\vec{\mu} \cdot \nabla B$ force on the neutrons,
- the ratio of gammas to neutrons is lower than at a reactor, and
- the prompt gamma background is separated in time from the neutrons of interest.

Not only does LANSCE provide the most intense such source, it is the only intense pulsed neutron facility at which proposals for nuclear physics experiments are entertained.

The Los Alamos staff associated with this effort is uniquely qualified to carry out the proposed work. The principal investigator, David Bowman is a world expert in precise parity violation experiments. He has measured parity violation in the nucleon-nucleon system as well as in neutron resonances with pulsed neutrons. Steve Lamoreaux and Geoff Greene have between them more than three decades of experience in a wide variety of precise measurements with cold neutrons. Seppo Penttilä has extensive experience in measurements of fundamental symmetries and is a world expert in cryogenic techniques for nuclear physics experiments. Scott Wilburn has participated in precise parity violation experiments using charged particles. Vincent Yuan has extensive experience with pulsed neutron experiments. In addition, as can be seen in appendix C, the rest of the collaboration is extremely experienced in studies of fundamental symmetries with low-energy neutrons.